# BEST AVAILABLE IMAGES

Defective images within this document are accurate representations of the original documents submitted by the applicant.

Defects in the images may include (but are not limited to):

- BLACK BORDERS
- TEXT CUT OFF AT TOP, BOTTOM OR SIDES
- FADED TEXT
- ILLEGIBLE TEXT
- SKEWED/SLANTED IMAGES
- COLORED PHOTOS
- BLACK OR VERY BLACK AND WHITE DARK PHOTOS
- GRAY SCALE DOCUMENTS

## IMAGES ARE BEST AVAILABLE COPY.

**As rescanning documents *will not* correct images, please do not report the images to the Image Problem Mailbox.**

## Remarks

The October 23, 2003 Official Action has been carefully reviewed. In view of the amendments submitted herewith and the following remarks, favorable reconsideration and allowance of this application are respectfully requested.

At the outset, it is noted that a shortened statutory response period of three (3) months was set forth in the October 23, 2003 Official Action. The initial due date for response, therefore, is January 23, 2004.

The Examiner has rejected claims 82 and 89 under 35 U.S.C. §112, second paragraph for alleged indefiniteness. Specifically, it is the Examiner's position that the terms "post-translational" and "substrate" in claims 82 and 89, respectively, are indefinite.

The Examiner has also maintained the rejection of claims 78-80, 82-90, and 93 under 35 U.S.C. §102(e) as allegedly anticipated by U.S. Patent 6,410,255; claims 78, 79, 82-90, and 93 under 35 U.S.C. §102(b) as allegedly anticipated by U.S. Patent 5,795,729; and claims 78-93 under 35 U.S.C. §103(a) as allegedly unpatentable over U.S. Patents 6,410,255 and 5,795,729 in view of Haugland ("Handbook of Fluorescent Probes and Chemicals, 5th ed." (1992) Molecular Probes, pp. 90-93).

Claims 94 and 95 have been objected to as being dependent on a rejected claim. Applicants note, however, that claim 95 is in independent form and, therefore, not dependent on a rejected claim. The Examiner previously indicated in the March 10, 2003 Official Action that claim 95 is in condition for allowance and the claim has not been amended in the interim.

The foregoing constitutes the entirety of the rejections and objections raised in the October 23, 2003 Official Action. In light of the present claim amendments and the following remarks, the above-mentioned objection and rejection are respectfully traversed. No other issues are

pending in the present application.

No new matter has been introduced into this application by reason of any of the amendments presented herewith. Moreover, none of the present claim amendments is believed to constitute a surrender of any originally claimed subject matter, or a narrowing of the claims in order to establish patentability. The effect of these amendments is merely to make explicit that which was implicit in the claims as originally worded.

**CLAIMS 82 AND 89, AS AMENDED, FULLY SATISFY THE REQUIREMENTS OF 35 U.S.C. 112, SECOND PARAGRAPH**

In support of the 35 U.S.C. §112, second paragraph rejection of claims 82 and 89, the Examiner asserts that claim 82 is unclear due to the use of the phrase "post-translational modification" and claim 89 is vague because it is unclear which substrate in claim 78 is being referred to by the term "substrate" in claim 89.

It is the Examiner's position that a "post-translational modification" can only be performed on a peptide that has been translated from mRNA. Applicants continue to maintain that the term post-translational may refer to a particular class of modifications which may be performed on a peptide or protein regardless of the origin of the peptide or protein. However, in the interest of advancing prosecution of the instant application, Applicants have amended claim 82 to recite a "post-translational type modification" as per the Examiner's suggestion in the March 10, 2003 Official Action.

Applicants have also amended claim 89 to recite a "peptide substrate" as opposed to a "substrate" thereby eliminating the vagueness perceived by the Examiner in the claim. This amendment is also in line with the Examiner's suggestion in the March 10, 2003 Official Action.

In light of the foregoing, Applicants respectfully submit that any indefiniteness that may have been engendered

by the previous wording of claims 82 and 89 has been eliminated. Therefore, the rejection of claims 82 and 89 under 35 U.S.C. §112, second paragraph should be withdrawn.

**CLAIMS 78-93 ARE NOT ANTICIPATED BY U.S. PATENTS 6,410,255 AND 5,795,729 AND ARE NOT RENDERED OBVIOUS BY U.S. PATENTS 6,410,255 AND 5,795,729 IN VIEW OF HAUGLAND ET AL.**

The Examiner's 35 U.S.C. §102(e) rejection of claims 78-80, 82-90, and 93 as allegedly anticipated by U.S. Patent 6,410,255 and the 35 U.S.C. §102(b) rejection of claims 78, 79, 82-90, and 93 as allegedly anticipated by U.S. Patent 5,795,729 are fundamentally flawed and therefore untenable. The same is true of the 35 U.S.C. §103(a) rejection of claims 78-93 as allegedly unpatentable over U.S. Patents 6,410,255 and 5,795,729 in view of Haugland ("Handbook of Fluorescent Probes and Chemicals, 5th ed." (1992) Molecular Probes, pp. 90-93).

The Examiner notes that both U.S. Patents 6,410,255 and 5,795,729 disclose methods of monitoring protein modifications such as phosphorylation, methylation, glycosylation, prenylation, ubiquitination, sulfation ADP-ribosylation, and proteolysis by detecting the cleavage of modified peptides. The Examiner also notes that U.S. Patents 6,410,255 and 5,795,729 fail to monitor these protein modifications by means of changes in FRET due to conformational changes caused by the protein modification. However, it is the Examiner's position that the peptides described by U.S. Patents 6,410,255 and 5,795,729 **inherently** function in the same manner as the peptides of the instantly claimed invention.

According to the Examiner, the three issues that must be resolved in determining inherency are 1) the event must occur, not just probably; 2) the event must always occur; and 3) a person of ordinary skill should recognize the missing

information. Applicants submit that at least the first two of these three issues cannot be resolved so as to support a finding of unpatentability, based on the peptides disclosed in U.S. Patents 6,410,255 and 5,795,729.

Specifically, the Examiner alleges issue 1 supports the rejection, noting that "phosphorylation changes the conformational state of proteins and peptides." Additionally, the Examiner contends that because "the change in conformation accompanying the modification is a simple chemical process, it must necessarily occur whenever the modification occurs." It is the Examiner's position, based on this reasoning, that the requirement of issue 2, that the event must always occur, also supports this rejection.

First, Applicants submit that introductory texts in biochemistry and molecular biology teach that post-translational modification of proteins do not necessarily result in conformational changes. Indeed, Molecular Biology of the Cell (Alberts et al. (1994) Garland Publishing, NY, page 202) states that:

> "[b]ecause each phosphate group carries two negative charges, its addition to a protein **can** cause a structural change ... such a change occurring at one site in a protein **can** in turn alter the protein's conformation elsewhere." [Emphasis added.]

Clearly, even elementary textbooks teach that post-translational modifications do not "always" result in conformational changes, locally or globally, in the protein.

As a specific example, Applicants respectfully direct the Examiner's attention to the fact that the phosphorylation of isocitrate dehydrogenase from *E. coli* fails to result in any long-range conformational changes and causes only very minor localized conformational shifts (Hurley et al. (1990) J. Biol. Chem. 265:3599-3602). Hurley et al. compare the crystal structure of phosphorylated and unphosphorylated isocitrate dehydrogenase and determine that "no large scale

conformational changes" result from the phosphorylation event at Ser113 and that the only alterations that occur include: 1) a rotation of Tyr160 by 15°, 2) the shift of the loop consisting of residues 229-234 by an average of 0.16Å which is less than the estimated error in the structure (0.2Å), and 3) the shifts of the side chains of Ile159 and Lys199 by 0.2Å (abstract and pages 3599-3600). Because the remainder of the protein fails to undergo any conformational change, fluorescent probes attached to regions outside of the minor localized conformational changes noted above would fail to produce a change in the spacing of the fluorescent probes and therefore fail to produce a detectable change in fluorescence, as required by the instantly claimed invention.

Further in this regard, Applicants submit that many other proteins have been structurally characterized as undergoing no detectable conformational change upon phosphorylation. Ostedgaard et al. (PNAS (2000) 97:5657-5662) teach that the R8 domain (residues 708-831) from the cystic fibrosis transmembrane conductance regulator upon phosphorylation does not undergo any conformational changes that are detectable by circular dichroism (CD) (page 5660, Fig. 6A). Ostedgaard et al. also teach that this lack of conformational change is common among other regulatory domains such as the R domain of the kinase-inducible domain (KID) of cAMP-responsive element-binding protein (CREB) (page 5661). Indeed, Parker et al. (Mol. Cell. Biol. (1996) 16:694-703) demonstrate by "circular dichrosim and one-dimensional nuclear magnetic resonance analyses" that "KID assumes a disordered structure which is unaffected by Ser-133 phosphorylation (page 701). In yet another example, Lin et al. (FEBS Letters (2003) 554:253-256) show that inhibitor-2 (I2), an inhibitor of protein phosphatase-1 (PP1), fails to undergo any conformational change upon phosphorylation, as determined by nuclear magnetic resonance and circular dichroism spectroscopy (page 253). Lin et al. further add that such a result is not

unexpected because previous studies on the effects of phosphorylation on the conformation of protein reveal that while some phosphorylation events lead to conformational changes, other phosphorylation events have "no effect at all" on the conformation on the protein (page 255).

In light of the foregoing, Applicants submit that it is evident that phosphorylation does not always induce conformational changes within a protein or peptide. Additionally, even when a conformational change does occur, it may be localized to a select few residues. Therefore, residues outside these select few residues would experience no change in distance from other such residues upon phosphorylation of the peptide.

Thus, Applicants respectfully submit that the peptides of U.S. Patents 6,410,255 and 5,795,729 clearly fail to inherently have the properties required of the peptides of the instantly claimed invention. Therefore, Applicants respectfully request that the rejections of claims 78-80, 82-90, and 93 under 35 U.S.C. §102(e); claims 78, 79, 82-90, and 93 under 35 U.S.C. §102(b); and claims 78-93 under 35 U.S.C. §103(a) be withdrawn.

**CONCLUSION**

It is respectfully requested that the amendments presented herewith be entered in this application, since the amendments are primarily formal, rather than substantive in nature. Furthermore, these amendments are believed to clearly place the pending claims in condition for allowance. In any event, the claims as presently amended are believed to eliminate certain issues and better define other issues which would be raised on appeal, should an appeal be necessary in this case. These amendments were not presented earlier, because they adopt claim language by the Examiner which had not been regarded as patentably significant.

In view of the amendments presented herewith, and the foregoing remarks, it is respectfully urged that the objection and rejection set forth in the October 23, 2003 Official Action be withdrawn and that this application be passed to issue.

In the event the Examiner is not persuaded as to the allowability of any claim, and it appears that any outstanding issues may be resolved through a telephone interview, the Examiner is requested to telephone the undersigned attorney at the phone number given below.

Respectfully submitted,
DANN, DORFMAN, HERRELL AND SKILLMAN
A Professional Corporation

By Patrick J. Hagan
Patrick J. Hagan
PTO Registration No. 27,643

Telephone: (215) 563-4100
Facsimile: (215) 563-4044
Enclosures: Lin et al.
Parker et al.
Ostedgaard et al.
Hurley et al.

# Phosphorylation by glycogen synthase kinase of inhibitor-2 does not change its structure in free state

Ta-Hsien Lin[a,b], Yi-Chen Chen[c], Chia-lin Chyan[d], Li-huang Tsay[e], Tzu Chun Tang[b], Hao-Hsuan Jeng[e], Fang-Min Lin[b], Hsien-bin Huang[e,*]

[a] *Institute of Biochemistry, National Yang-Ming University, Shih-pai, Taipei 112, Taiwan, ROC*
[b] *Department of Medical Research and Education, Taipei Veterans General Hospital, Shih-pai, Taipei 112, Taiwan, ROC*
[c] *Department of Medical Technology, Tzu Chi University, Hualien 970, Taiwan, ROC*
[d] *Department of Chemistry, National Dong Hwa University, Hualien 974, Taiwan, ROC*
[e] *Institute of Molecular Biology, National Chung Cheng University, Chia-Yi 621, Taiwan, ROC*

Received 13 August 2003; revised 16 September 2003; accepted 18 September 2003

First published online 20 October 2003

Edited by Thomas L. James

**Abstract Inhibitor-2 (I2) is a thermostable protein that specifically binds to the catalytic subunit of protein phosphatase-1 (PP1), resulting in the formation of the inactive holoenzyme, ATP-Mg-dependent phosphatase. Phosphorylation of I2 at Thr-72 by glycogen synthase kinase-3 (GSK-3) results in activation of the phosphatase, suggesting that kinase action triggers conformational change in the complex. In this paper, we characterize the effect of GSK-3 phosphorylation on the structure of free state I2[1–172] by nuclear magnetic resonance and circular dichroism spectroscopy, and show that phosphorylation has no significant effect on its conformation. We conclude that the conformational changes of ATP-Mg-dependent phosphatase induced by GSK-3 phosphorylation must depend on the interactions between PP1 and I2.**


*Key words:* Nuclear magnetic resonance; Circular dichroism; Inhibitor-2; Protein phosphatase-1; Glycogen synthase kinase-3

## 1. Introduction

Protein phosphatase-1 (PP1), one of the major mammalian serine/threonine protein phosphatases, plays a critical role in the regulation of various cellular functions, including carbohydrate metabolism, protein synthesis, cell cycle, muscle contraction and neuronal signaling [1–4]. PP1 occurs in cells as a holoenzyme and consists of a 37-kDa catalytic subunit combined with a specific regulatory subunit that appears to target the enzyme to specific subcellular compartments. The catalytic subunit of PP1 is also regulated by several thermostable protein inhibitors, including inhibitor-1, DARPP-32 and inhibitor-2 (I2). PP1 is only inhibited by inhibitor-1 and DARPP-32 when both inhibitors are pre-phosphorylated by cAMP-dependent protein kinase (PKA); by contrast, PP1 is inhibited by I2 without pre-phosphorylation. I2 binds to PP1 to form a complex that is the ATP-Mg-dependent form of the phosphatase, and in turn inhibits enzyme activity. This inactive holoenzyme can be reactivated when glycogen synthase kinase-3 (GSK-3) phosphorylates I2 at Thr-72. The mechanism for reactivation of ATP-Mg-dependent phosphatase is complicated. GSK-3 phosphorylation does not induce the dissociation of the complex, but triggers a conformational change in PP1, which rapidly auto-dephosphorylates the phosphorylated Thr-72 site of I2. Subsequently, the inactive holoenzyme is slowly converted into an active form [5]. In its dephosphorylated form, the active complex then slowly recurs to an inactive state. Different stages of the reactivation cycle are carried out by diverse regions of I2 [6]. However, it remains uncertain whether or not GSK-3 phosphorylation pre-triggers a conformational change in I2, in turn leading to the structural change of the phosphatase complex. To investigate the conformational state of I2, we prepared GSK-3-phosphorylated I2[1–172] and characterized its structure by nuclear magnetic resonance (NMR) and circular dichroism (CD) spectroscopy. Our results suggest that GSK-3 phosphorylation does not significantly change the structure of I2 in the free state. The interactions between PP1 and I2 may play a vital role in the conformational change of the complex upon GSK-3 phosphorylation.

## 2. Materials and methods

### 2.1. Proteins and reagents

ATP, Tris, dithiothreitol, EDTA, Brij-35 and sodium azide were obtained from Sigma. $^{15}NH_4Cl$ and [$^{13}$C]glucose were purchased from Cambridge Isotope Laboratories. Recombinant GSK-3β was prepared from *Escherichia coli* as described [7]. One unit of GSK-3β was defined as the amount of enzyme that incorporates 1 nmol of phosphate/min into a PKA-pre-phosphorylated peptide (KRREILSRRPS(P)YR) at 50 μM.

### 2.2. Preparation of GSK-3-phosphorylated $^{15}$N-enriched I2[1–172]

Human recombinant $^{15}$N-enriched I2[1–172] was prepared as described [8]. I2[1–172] showed similar properties to wild-type I2 with respect to the $IC_{50}$ for inhibition of PP1, the formation of an inactive complex with PP1 and re-activation of PP1 following phosphorylation by GSK-3β (data not shown). Phosphorylation of $^{15}$N-enriched I2[1–172] by GSK-3β was performed in 50 mM Tris–HCl buffer, pH 7.0, containing 0.1 mM EDTA, 0.02% sodium azide, 0.05% Brij-35, 0.2 mM ATP, 2.5 mM magnesium acetate, $^{15}$N-enriched I2[1–172] (5 mg/ml) and GSK-3β (2 U/ml). The reaction was carried out at 30°C for 2 days, with fresh GSK-3β (2 U/ml) and ATP (0.2 mM final concentration) added every 12 h. $^{15}$N-enriched phospho-I2[1–172] was purified by FPLC using a Mono-Q column (10/10) with a linear salt gradient from 0.18 to 0.42 M NaCl in 20 mM Tris–HCl buffer, pH 7.5, containing 0.2 mM EDTA, 2.0 mM dithiothreitol and 0.02% (w/v) sodium azide. Fractions (1.5 ml/tube) were collected from 0 to

*Corresponding author.
*E-mail address:* biohbh@ccu.edu.tw (H.-b. Huang).

0014-5793/03/$22.00 
doi:10.1016/S0014-5793(03)01097-4

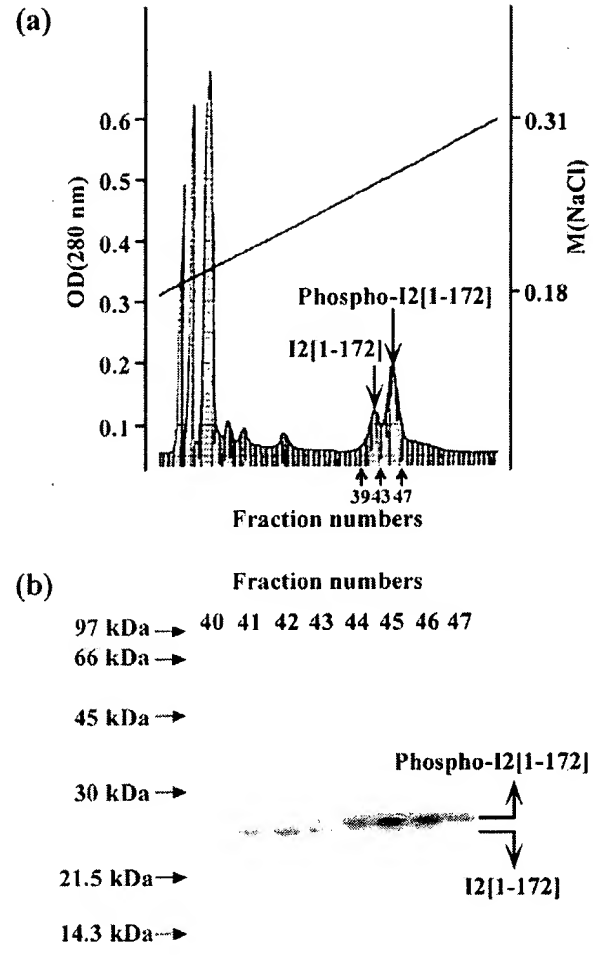


Fig. 1. a: Purification of phospho-I2[1–172] by FPLC on a Mono-Q column. b: SDS–PAGE analysis of phospho-I2[1–172] in fractions 40–47 from panel a. Molecular weight markers are phosphorylase b (97 kDa), bovine serum albumin (76 kDa), ovalbumin (45 kDa), carbonic anhydrase (30 kDa), trypsin inhibitor (21.5 kDa), and lysozyme (14.3 kDa).

45 min. The fractions containing phospho-protein were pooled, dialyzed against water to remove the excess reagents and lyophilized to powder.

### 2.3. NMR spectroscopy

For NMR spectroscopy, samples of 0.5 mM $^{15}$N-enriched phospho-I2[1–172] in 90% $H_2O$/10% $D_2O$ were prepared in 100 mM phosphate buffers, pH 6.0, with 0.02% $NaN_3$. 2,2-Dimethyl-2-silapentane-5-sulfonic acid was used as the internal chemical shift standard [9,10]. The final protein sample solution was transferred to a 5-mm Shigemi NMR tube (Shigemi, Tokyo, Japan) to record the NMR spectra. 2D $^1$H-$^{15}$N-heteronuclear single-quantum coherence (HSQC) spectra were recorded at 296 K on a Bruker AVANCE-500 spectrometer equipped with a 5-mm inverse triple resonance ($^1$H/$^{13}$C/BB), $z$-axis gradient probe. Water suppression was achieved by applying WATERGATE sequence [11]. Quadrature detection in the indirectly detected dimension was accomplished using the States-TPPI method [12]. Spectral width was 1500 Hz in both the direct ($^1$H) and indirect ($^{15}$N) dimensions. A total of 128 time increments were recorded with 32 transients for each increment. Spectra were processed using XWINNMR and analyzed using AURELIA [13] on an SGI workstation.

### 2.4. CD spectroscopy

CD spectra were recorded using a Jasco 715 spectropolarimeter with a thermal circulator accessory. The optical rotation was calibrated using d-10-camphorsulfonic acid at wavelengths of 192.5 and 290 nm. The wavelength was calibrated with benzene vapor. All measurements were performed in quartz cells with a path length of 0.01 cm. The protein concentration of the samples was 1.0 mg/ml. Data were collected for wavelengths from 190 to 260 nm at 1-nm increments. Reported CD spectra represent the average of at least three individual samples and three repeated measurements of each sample. Baseline corrections for the spectra were made by using solutions containing DMPC. All measurements were carried out at 25.0 ± 0.2°C. Secondary structure analysis was performed using online software, website: Dichroweb from BBRC Centre for Protein and Membrane Structure and Dynamics [14,15].

## 3. Results

### 3.1. Phosphorylation of $^{15}$N-enriched I2[1–172] by GSK-3β

The two rat brain isoforms of GSK-3, GSK-3α and GSK-3β, differ in their ability to phosphorylate I2 at Thr-72 [16,17]. GSK-3β is a better I2 kinase than GSK-3α. Under the present experimental conditions, however, the yield of phosphorylated I2 by GSK-3β was low. Therefore, both fresh GSK-3β and ATP were added every 12 h during the phosphorylation reaction. After 2 days, about 70% of the $^{15}$N-enriched I2[1–172] was phosphorylated, as judged by analysis of the ion exchange chromatography fractions (Fig. 1a). Sodium dodecyl sulfate–polyacrylamide gel electrophoresis (SDS–PAGE) shows that $^{15}$N-enriched phospho-I2[1–172] has a lower mobility on the gel (Fig. 1b), and that phospho-I2[1–172] was purified to greater than 96% homogeneity by FPLC using a Mono-Q column (data not shown).

The effect of phosphorylation on the conformational behavior of I2[1–172] was studied by CD spectroscopy. Fig. 2 shows an overlay of the CD spectra of I2[1–172] and phospho-I2[1–172]. These two spectra are almost identical, suggesting that the global conformation of I2[1–172] is not influenced by phosphorylation. Analysis of the secondary structure from the CD spectra shows that both I2[1–172] and phospho-I2[1–172] have a mostly non-structural conformation. The NMR results (Fig. 3) also support this inference. Clearly, the chemical shifts of the backbone amides and the $^{15}$N resonances for most of the residues of I2[1–172] remain unchanged when Thr-72 is phosphorylated by GSK-3. Working from previously assigned backbone amide proton and $^{15}$N

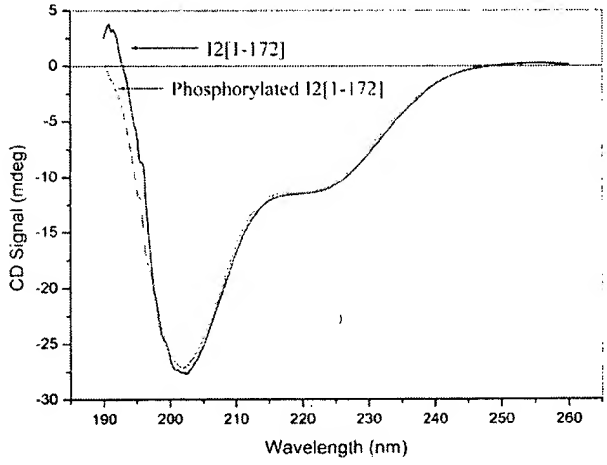


Fig. 2. An overlay of the CD spectra of I2[1–172] (black) and phosphorylated I2[1–172] (red).

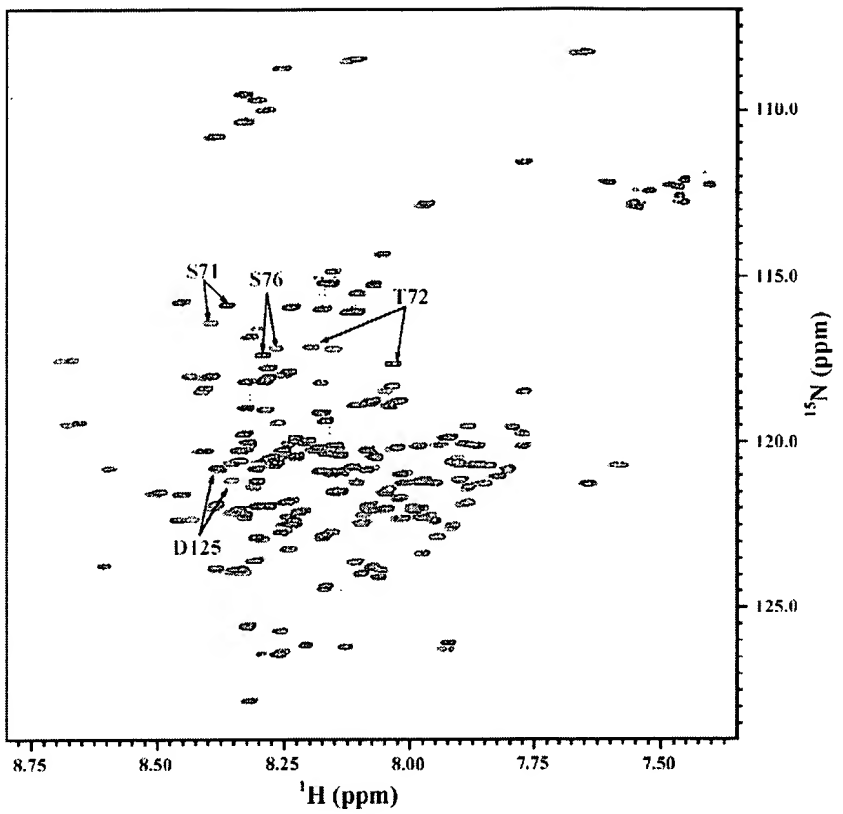


Fig. 3. An overlay of the 2D $^{1}$H-$^{15}$N-HSQC spectra of I2[1–172] (black) and phosphorylated I2[1–172] (red). Residues with significant chemical shift changes are labeled.

chemical shifts of I2[1–172] [8], residues with significant chemical shift changes (S71, T72, S76, D125) were identified by a graphic mapping approach. The chemical shift changes of these residues may be due to the electrostatic effect of the phosphate group or to phosphorylation-induced conformational change or to a combination of both [18]. Since only a few residues exhibit significant chemical shift changes, it is unlikely that phosphorylation of I2[1–172] at Thr-72 has a significant effect on the global conformation of I2[1–172]. Besides, these residues are randomly distributed in the primary sequence, and not located consecutively, which suggests that even local conformational changes would probably occur. Our interpretation of the results is therefore that the phosphorylation-induced chemical shift changes are mainly caused by the through-space electrostatic effects of the phosphate group. If this is correct, then the residues with significant chemical shift changes should be located in the spatial vicinity of the phosphorylation site.

## 4. Discussion

Previous studies on the effect of phosphorylation on the conformation of proteins have yielded diverse results [19–23], with some supporting a change of conformation and others reporting no effect at all. In most cases, when phosphorylation causes conformational change, long-term allosteric changes may occur [19–22]. In the case of I2, the conformation of which is a random coil except for a short α-helix that spans the region from residue 132 to 142 [8], our NMR and CD spectroscopy data suggest that no significant conformational changes were induced after the Thr-72 site of I2[1–172] was phosphorylated by GSK-3. Using fluorescence techniques, Picking et al. [5] demonstrated that phosphorylation by GSK-3 resulted in a conformational change of I2, but this effect was induced only when I2 had formed a complex with PP1. Furthermore, they pointed out that the free phosphorylated I2 will eventually relax back to its native conformational state. Bearing in mind that our NMR and CD data were obtained for I2 in its free state and in equilibrium, the present results are consistent with those of Picking et al. [5]. We conclude that the binding of I2 to PP1 is critical, and that the interactions between PP1 and I2 may play a vital role in the conformational change of the complex upon GSK-3 phosphorylation.

*Acknowledgements:* This work was supported by the National Science Council of the Republic of China (NSC91-2311-B-010-002 and NSC92-2320-B-194-005) and the Taipei Veterans General Hospital, Taiwan, Republic of China.

## References

[1] Cohen, P. (1989) Annu. Rev. Biochem. 58, 453–508.
[2] Shenolikar, S. and Nairn, A.C. (1991) Adv. Second Messenger Phosphoprotein Res. 23, 1–121.
[3] Shenolikar, S. (1994) Annu. Rev. Cell Biol. 10, 55–86.
[4] Wera, S. and Hemmings, B.A. (1995) Biochem. J. 311, 17–29.
[5] Picking, W.D., Kudlicki, W., Kramer, G., Hardesty, B., Vandenheede, J.R., Merlevede, W., Park, I.K. and DePaoli-Roach, A. (1991) Biochemistry 30, 10280–10287.

[6] Park, I.K. and DePaoli-Roach, A.A. (1994) J. Biol. Chem. 269, 28919–28928.
[7] Wang, Q.M., Fiol, C.J., DePaoli-Roach, A.A. and Roach, P.J. (1994) J. Biol. Chem. 269, 14566–14574.
[8] Huang, H.B., Chen, Y.C., Tsai, L.H., Wang, H.C., Lin, F.M., Horiuchi, A., Greengard, P., Nairn, A.C., Shiao, M.S. and Lin, T.H. (2000) J. Biomol. NMR 17, 359–360.
[9] Wishart, D.S., Bigam, C.G., Yao, J., Abildgaard, F., Dyson, H.J., Oldfiels, E., Markley, J.L. and Sykes, B.D. (1995) J. Biomol. NMR 6, 135–140.
[10] Wishart, D.S. and Sykes, B.D. (1994) Methods Enzymol. 239, 363–392.
[11] Piotto, M., Saudek, V. and Sklenar, V. (1992) J. Biomol. NMR 2, 661–665.
[12] Marion, D., Ikura, M., Tschudin, R. and Bax, A. (1989) J. Magn. Reson. 85, 393–399.
[13] Neidig, K.-P., Geyer, M., Gorler, A., Antz, C., Saffrich, R., Beneike, W. and Kalbitzer, R. (1995) J. Biomol. NMR 6, 255–270.
[14] Lobley, A. and Wallace, B.A. (2001) Biophysical J. 80, 373a.
[15] Lobley, A. and Whitmore, L. (2002) Bioinformatics 18, 211–212.
[16] Woodgett, J.R. (1990) EMBO J. 9, 2431–2438.
[17] Wang, Q.M., Park, I.K., Fiol, C.J., Roach, P.J. and DePaoli-Roach, A.A. (1994) Biochemistry 33, 143–147.
[18] Radhakrishnan, I., Perez-Alvarado, G.C., Dyson, H.J. and Wright, P.E. (1998) FEBS Lett. 430, 317–322.
[19] Johnson, L.N. and O'Reilly, M. (1996) Curr. Opin. Struct. Biol. 6, 762–769.
[20] Russo, A., Jeffrey, P.D. and Pavletich, N.P. (1996) Nat. Struct. Biol. 3, 696–700.
[21] Lin, K., Rath, V.L., Dai, S.C., Fletterick, R.J. and Hwang, P.K. (1996) Science 273, 1539–1541.
[22] Birck, C., Mourey, L., Gouet, P., Fabry, B., Schumacher, J., Rousseau, P., Kahn, D. and Samama, J.-P. (1999) Structure 7, 1505–1515.
[23] Seavers, P.R., Lewis, R.J., Brannigan, J.A., Verschueren, K.H.G., Murshudov, G.N. and Wilkinson, A.J. (2001) Structure 9, 605–614.

MOLECULAR AND CELLULAR BIOLOGY, Feb. 1996, p. 694–703
0270-7306/96/$04.00+0

Vol. 16, No. 2

# Phosphorylation of CREB at Ser-133 Induces Complex Formation with CREB-Binding Protein via a Direct Mechanism

D. PARKER,[1] K. FERRERI,[1] T. NAKAJIMA,[1] V. J. LAMORTE,[2] R. EVANS,[2]
S. C. KOERBER,[1] C. HOEGER,[1] AND M. R. MONTMINY[1]*

*The Clayton Foundation Laboratories for Peptide Biology[1] and Gene Expression Laboratory,[2] The Salk Institute, La Jolla, California 92037*

Received 13 October 1995/Returned for modification 10 November 1995/Accepted 15 November 1995

**We have characterized a phosphoserine binding domain in the coactivator CREB-binding protein (CBP) which interacts with the protein kinase A-phosphorylated, and hence activated, form of the cyclic AMP-responsive factor CREB. The CREB binding domain, referred to as KIX, is α helical and binds to an unstructured kinase-inducible domain in CREB following phosphorylation of CREB at Ser-133. Phospho-Ser-133 forms direct contacts with residues in KIX, and these contacts are further stabilized by hydrophobic residues in the kinase-inducible domain which flank phospho-Ser-133. Like the src homology 2 (SH2) domains which bind phosphotyrosine-containing peptides, phosphoserine 133 appears to coordinate with a single arginine residue (Arg-600) in KIX which is conserved in the CBP-related protein P300. Since mutagenesis of Arg-600 to Gln severely reduces CREB-CBP complex formation, our results demonstrate that, as in the case of tyrosine kinase pathways, signal transduction through serine/threonine kinase pathways may also require protein interaction motifs which are capable of recognizing phosphorylated amino acids.**

A number of signaling pathways have been shown to regulate the expression of target genes by inducing the phosphorylation of specific transcription factors (9). The second messenger cyclic AMP (cAMP), for example, stimulates the expression of numerous genes through protein kinase A (PKA)-dependent phosphorylation of CREB at Ser-133 (7). Although phosphorylation may regulate such factors by enhancing their nuclear targeting or DNA binding activities, CREB belongs to a group of proteins whose transactivation potential is specifically affected (2, 8).

The CREB transactivation domain is bipartite, consisting of a kinase-inducible domain (KID) (amino acids [aa] 88 to 160) and a glutamine-rich constitutive activator termed Q2 (aa 161 to 283) which synergize to stimulate target gene expression in response to cAMP (2). When fused to a heterologous DNA binding domain such as that of GAL4, the KID can cooperate in *trans* not only with Q2 but also with a number of constitutive activators, including GAL4 and VP16. These observations suggest that the KID contains the minimal region which is both necessary and sufficient for PKA-regulated activity.

We and others have recently characterized a 265-kDa CREB-binding protein (CBP) which binds to CREB in a phosphorylation-dependent manner in vitro (4) and which is closely related to the E1A-associated protein P300 (6). CBP appears to be important for cAMP-responsive transcription, as illustrated by microinjection studies in which anti-CBP antiserum could block transcription from a cAMP-responsive promoter and by transfection studies in which a CBP expression vector could potentiate CREB activity in a phosphorylation-dependent manner (1, 11). It is not known, however, whether Ser-133 phosphorylation allows CREB to associate with CBP via an allosteric mechanism or a direct mechanism or whether the CREB-CBP interaction is in fact critical for cAMP-responsive transcription in vivo. Here we characterize a domain in CBP, termed KIX, which binds to the KID of CREB in a phospho-Ser-133-dependent manner. Our results suggest that KIX represents a novel motif which promotes protein-protein interactions in response to Ser/Thr kinase-mediated signals.

* Corresponding author. Mailing address: The Clayton Foundation Laboratories for Peptide Biology, The Salk Institute, 10010 North Torrey Pines Rd., La Jolla, CA 92037.

## MATERIALS AND METHODS

**Binding assays.** Glutathione *S*-transferase (GST) fusion proteins were expressed in pGEX-KT and purified as previously described (4). Recombinant CREB protein was labeled with [γ-$^{32}$P]ATP by using the purified catalytic subunit of PKA (PKA-Cα; a generous gift from S. Taylor) in a reaction volume of 25 μl [25 mM Tris-HCl (pH 7.0), 10 mM $MgCl_2$, 2 mM ethylene glycol-bis(β-aminoethyl ether)-*N,N,N',N'*-tetraacetic acid (EGTA), 1 mM dithiothreitol, 0.1 mg of bovine serum albumin (BSA) per ml, 1 mM phenylmethylsulfonyl fluoride, 0.5 μg of leupeptin per ml] for 1 h at 30°C. Free [$^{32}$P]ATP was removed by centrifugation through Centri-Sep columns (Princeton Separations, Inc.). Binding assays were performed in PC+100 buffer (20 mM *N*-2-hydroxyethylpiperazine-*N'*-2-ethanesulfonic acid [HEPES] [pH 7.9], 100 mM KCl, 0.2 mM EDTA, 5 mM $MgCl_2$, 0.1% Nonidet P-40, 20% glycerol, 0.1 mg of BSA per ml, 1 mM phenylmethylsulfonyl fluoride). Labeled CREB was mixed with GST fusion proteins in 100-μl reaction volumes and incubated for 30 min at room temperature. Glutathione-Sepharose (20 μl of a 50% slurry) was added, and the mixture was incubated at room temperature with a rotator. Samples were washed three times with PC+100 buffer and then analyzed by sodium dodecyl sulfate-polyacrylamide gel electrophoresis (SDS-PAGE). $^{32}$P-labeled CREB bands were quantified by PhosphorImager analysis.

**Cross-linking assays.** A CREB peptide consisting of aa 121 to 151 ($CREB_{121-151}$) was phosphorylated by PKA-Cα with either γ-$^{35}$S-ATP or [$^{32}$P]ATP in 20 mM Tris-HCl (pH 7.0)–10 mM $MgCl_2$–1 mM EDTA. For cross-linking, 6 pmol of phosphopeptide was preincubated in 20 μl of 20 mM sodium phosphate (pH 7.4)–100 mM KCl–2 mM $MgCl_2$–0.2 mM EDTA–0.05% Nonidet P-40–20% glycerol in the presence and in the absence of 1 mM $K_2PtCl_4$. After 10 min at room temperature, 1 nmol of the KIX S/B polypeptide (aa 553 to 679 of CBP) was added and allowed to react for 30 min at room temperature. The reaction was stopped by the addition of 1 volume of 2× nonreducing SDS loading buffer, and the resulting mixture was boiled for 1 min and electrophoresed on an SDS–15% polyacrylamide gel.

**Circular dichroism studies.** The $CREB_{88-160}$ peptide and KIX S/B were expressed in *Escherichia coli* with the pGEX-2T vector (Pharmacia) and purified on glutathione-Sepharose according to the supplier's instructions. After phosphorylation of $CREB_{88-160}$ with recombinant PKA-Cα (kindly provided by S. Taylor, University of California, San Diego), the samples were exchanged into 10 mM sodium phosphate (pH 7.4) and concentrated. For absorbance measurements, the samples were diluted to final concentrations of 5 μM peptide and 0.67 mM sodium phosphate, and the spectra were measured on an Aviv 60DS circular dichroism spectrometer with a 0.1-cm cuvette. Secondary structure was estimated from the data by using the PROSEC program.

**Screening for mutant KIX cDNAs.** Random mutations in the KIX domain of CBP were made by a modified PCR technique as described by Leung et al. (12). Following amplification, the PCR products were ligated into the pCRII-TA cloning vector (Invitrogen), transformed into One Shot cells, and plated. Bacterial colonies were then streaked onto isopropyl-β-D-thiogalactopyranoside (IPTG)-treated nitrocellulose filters and incubated overnight at 37°C. The colonies were then exposed to chloroform for 15 min and lysed in 100 mM Tris-HCl (pH 8.0)–150 mM NaCl–5 mM $MgCl_2$–1% SDS for 10 min on a rotator. After two washes in TNT buffer (10 mM Tris-HCl [pH 8.0], 150 mM NaCl, 0.05% Tween 20), the filters were incubated for 1 h in blocking buffer (1× phosphate-buffered saline [PBS], 5% nonfat dried milk, 1% BSA, 0.1% Triton X-100). The filters were then incubated with $^{32}$P-labeled CREB for 2 h in buffer A (10 mM Tris [pH 7.5], 100 mM NaCl, 5 mM $MgCl_2$, 1 mM dithiothreitol, 0.5% BSA, 5% nonfat dried milk, 0.1% Triton X-100, 1 mM EDTA, 5% glycerol) and subsequently washed twice for 30 min each time in buffer A. The filters were exposed to Kodak XAR film, and colonies which did not bind phospho-CREB were identified. The corresponding cDNAs were sequenced on both strands.

**Phosphatase protection assays.** $^{32}$P-labeled CREB (0.25 pmol) was mixed with 100 pmol of GST fusion proteins in a total volume of 60 μl of phosphatase buffer (20 mM HEPES [pH 7.0], 100 mM KCl, 0.1 mg of BSA per ml, 1 mM dithiothreitol, 7 mM $MgCl_2$, 1 mM $MnCl_2$, 1 mM phenylmethylsulfonyl fluoride, 5 ng of leupeptin per ml). After 30 min of incubation at 37°C, protein phosphatase 2A (PP2A) (0.2 μg, kindly provided by G. Walter) was added to each sample, and CREB dephosphorylation was allowed to proceed at 37°C. Time point samples were collected at 15-min intervals up to 2 h, and reactions were terminated by addition of SDS loading buffer. The samples were loaded onto SDS-polyacrylamide gels and exposed to X-ray film.

**Microinjection assays.** NIH 3T3 cells were cultured in 7.5% $CO_2$ in Dulbecco modified Eagle medium containing 10% calf serum. To facilitate microinjection, cells were plated on scored glass coverslips and made quiescent by serum deprivation. The cells were placed in Dulbecco modified Eagle medium containing 0.05% calf serum for 24 to 48 h prior to microinjection. The cells were microinjected with an Eppendorf semiautomated microinjection system that delivers ~$10^{-15}$ liters per cell. The pCRE-β-galactosidase reporter construct (200 ng/μl) (14) was injected along with a marker rabbit immunoglobulin G (IgG). The M4B and KIX peptides were injected at equal concentrations of 5 mg/ml. M4B is a mutant KIX peptide, identified by PCR mutagenesis screening, with the inactivating point mutations I-611→T and Y-650→N. After injection, cells were immediately stimulated with 10 μM forskolin and 0.5 mg of 3-isobutyl-1-methylxanthine (IBMX) per ml for 2 h to induce cAMP-dependent transcription. Subsequently, cells were fixed in 3.7% formaldehyde–PBS, permeabilized with 0.3% Triton X-100, and immunostained with donkey anti-rabbit IgG–fluorescein isothiocyanate (1:200) (Jackson Laboratories) to detect injected cells. Cells that contained a blue precipitate were scored positive. As a control, cells were microinjected with a constitutive expression construct, pCMX-β-galactosidase (100 ng/μl), and the KIX peptide at the same concentration as above (5 mg/ml). Two hours after injection, the cells were fixed and stained as described above.

## RESULTS

**An α-helical domain in CBP binds to phospho-Ser-133 CREB.** To identify a minimal domain in CBP which is both necessary and sufficient for interaction with CREB phosphorylated at Ser-133 (phospho-Ser-133 CREB), we prepared a series of recombinant polypeptides (4) (Fig. 1A). In GST pull-down assays, a 94-aa fragment of CBP (KIX 10.4) extending from aa 586 to 679 of CBP was sufficient for high-affinity phospho-CREB binding activity. Further carboxy-terminal truncation of the KIX polypeptide to residue 661 (KIX 5.6 [aa 576 to 661]) lowered the binding affinity of KIX for phospho-Ser-133 CREB three- to fourfold (Fig. 1B). N-terminal deletion to aa 616 similarly reduced complex formation. Thus, 94 residues in KIX (aa 586 to 679) appear to be required for phospho-CREB recognition, a result which is further supported by sequence alignment data revealing that CBP, its paralog P300, and a related protein in *Caenorhabditis elegans* (R10e11.1) have strong sequence identity in that region (not shown). In parallel binding assays, we determined that the KIX-related region of P300 could indeed associate with phospho-Ser-133 CREB (not shown).

Previous studies demonstrating that the 72-aa KID in CREB is both necessary and sufficient for transcriptional induction by cAMP prompted us to test this domain for interaction with CBP (Fig. 1C). In solution binding assays, a recombinant KID polypeptide (aa 88 to 160), phosphorylated in vitro at Ser-133 with PKA, interacted strongly with CBP (Fig. 1C, lane 2). But the unphosphorylated KID did not bind to CBP (Fig. 1C, lane KID), demonstrating that formation of this complex is also phospho-Ser-133 dependent.

To examine the structural basis for interaction between CBP and CREB, we performed circular dichroism studies of the KIX and KID peptides (Fig. 1D). The KIX domain in CBP appeared to be α helical, as indicated by a maximum at 194 nm and two minima at 207 and 223 nm. By contrast, the KID in CREB showed no evidence of ordered structure, as revealed by a minimum at 203 nm. And PKA phosphorylation at Ser-133 had no effect on the circular dichroism spectrum of the KID, suggesting that phosphorylation does not induce structural changes in the KID. This result is supported by preliminary one-dimensional nuclear magnetic resonance studies of the KID in CREB which suggest that the KID is largely unstructured in both the unphosphorylated and phosphorylated states (14a).

**Hydrophobic interactions contribute to CREB-CBP complex formation.** To identify individual residues in the KIX polypeptide which are important for interaction with CREB, we developed a colony binding assay (Fig. 2). Using $^{32}$P-labeled CREB as a probe, we detected specific binding to bacterial colonies which expressed recombinant KIX protein but not to colonies expressing unrelated proteins. By employing a random PCR mutagenesis protocol, we generated point mutations within the KIX domain (aa 455 to 679) and identified mutant KIX cDNAs which expressed the full-length KIX polypeptide when purified by glutathione-Sepharose chromatography but did not bind Ser-133 phospho-CREB in vitro (Fig. 2B). Sequence analysis of these phospho-CREB binding mutants revealed a cluster of amino acid substitutions occurring primarily at conserved hydrophobic residues from aa 591 to 620 of the KIX domain. On the basis of the helicity predicted for KIX by circular dichroism spectroscopy, most of these hydrophobic residues appear to occupy one face of an amphipathic α helix.

To determine whether hydrophobic interactions are important for complex formation between CBP and phospho-Ser-133 CREB, as predicted from the mutagenesis studies, we examined the stability of this complex in the presence of increasing concentrations of NaCl (Fig. 2D). Binding of phospho-CREB to a GST-KIX affinity resin was stable at high concentrations of salt (500 mM NaCl) (Fig. 2D) but was readily disrupted by a nonionic detergent (0.1% deoxycholate) (Fig. 2E). These results support the proposal that hydrophobic interactions contribute importantly to the formation of the CREB-CBP complex. In this regard, the KID in CREB (aa 88 to 160) also contains a number of hydrophobic residues which flank the Ser-133 phosphoacceptor site and which are conserved in the CREB family members CREM and ATF1. Whereas the wild-type phospho-Ser-133 KID could bind with high affinity to GST resins containing the KIX S/B polypeptide (Fig. 2F, left panel, lane KIX S/B), a mutant KID peptide containing Ile-137–Leu-138 to Ala-137–Ala-138 substitutions could not (Fig. 2F, right panel, lane KIX S/B). These results indicate that hydrophobic residues flanking phospho-Ser-133 are indeed important for complex formation.

**The KIX polypeptide is recruited to cAMP-responsive promoters and blocks cAMP-responsive transcription in vivo.** To determine whether we could visualize phosphorylation-dependent recruitment of KIX to a cAMP-responsive promoter, we performed gel shift assays using a double-stranded cAMP-responsive element (CRE) oligonucleotide (Fig. 3A and B). Addition of the KIX polypeptide to reaction mixtures containing phospho-Ser-133 CREB and a $^{32}$P-labeled CRE generated

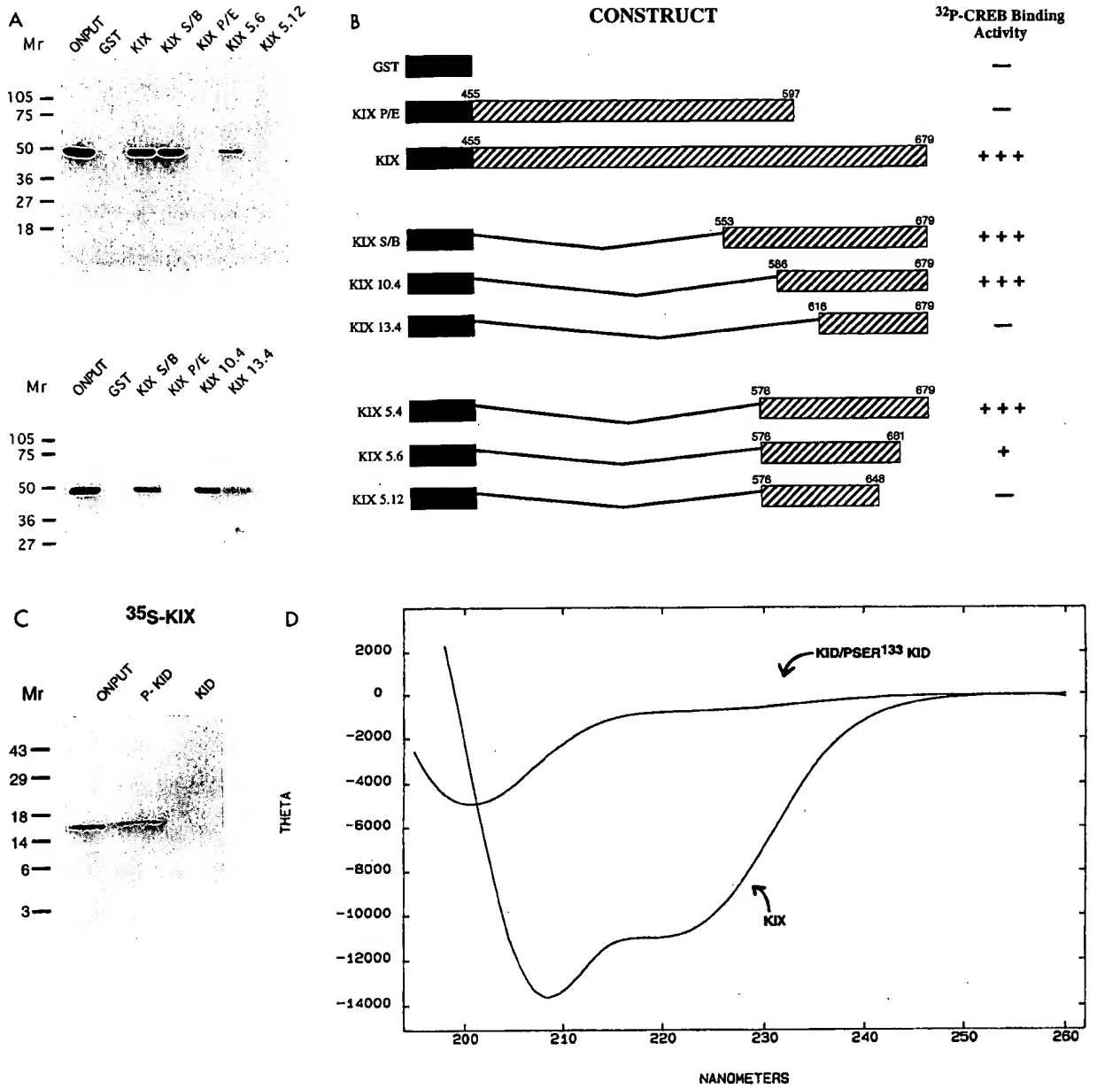


FIG. 1. The KIX region in CBP is an α-helical domain which binds to the KID of CREB in a phospho-Ser-133-dependent manner. (A and B) Characterization of domains in CREB and CBP which are necessary and sufficient for phosphorylation-dependent association in vitro. (A) GST pull-down assay of $^{32}$P-labeled CREB phosphorylated at Ser-133 in vitro with PKA. Lanes: ONPUT, $^{32}$P-labeled CREB added to each resin; GST, control resin containing GST alone; KIX, GST affinity resin expressing a CBP fragment consisting of aa 455 to 679; KIX S/B, GST affinity resin expressing a CBP fragment consisting of aa 553 to 679; KIX P/E, GST affinity resin expressing a CBP fragment consisting of aa 455 to 597; KIX 5.6, GST affinity resin expressing a CBP fragment consisting of aa 576 to 661; KIX 5.12, GST affinity resin expressing a CBP fragment consisting of aa 576 to 648; KIX 10.4, GST affinity resin expressing a CBP fragment consisting of aa 586 to 679; KIX 13.4, GST affinity resin expressing a CBP fragment consisting of aa 616 to 679. Mr, relative molecular weight in thousands. (B) Summary of deletional analysis of the KIX domain by GST pull-down assays. +++, 50 to 100% of wild-type binding activity; ++, 15 to 50% of wild-type binding activity; +, 5 to 15% of wild-type binding activity; −, no binding activity. Inclusive amino acid endpoints for each construct are indicated. (C) Pull-down assay of purified recombinant $^{35}$S-labeled KIX S/B polypeptide. Lanes: ONPUT, $^{35}$S-labeled KIX added to each resin; P-KID, retention of KIX on resin containing Ser-133-phosphorylated KID peptide (aa 88 to 160); KID, retention of KIX on resin containing unphosphorylated KID peptide. (D) Structure of the KID and the KIX domain in vitro. Circular dichroism spectra of purified KIX S/B (aa 553 to 679) and phospho-Ser-133 KID (aa 88 to 160) polypeptides are shown. The spectra are plotted as molar ellipticity (THETA) versus wavelength in nanometers. α-helical content was estimated by PROSEC analysis (3).

a complex which migrated more slowly than the phospho-CREB–CRE complex (Fig. 3A; compare lanes 1 and 5). But addition of the KIX polypeptide to reaction mixtures containing unphosphorylated CREB had no effect on the mobility of the CREB-CRE complex (Fig. 3A; compare lanes 1 and 6), suggesting that KIX is recruited to cAMP-responsive promoter elements in a phospho-Ser-133-dependent manner. Moreover, CREB binding mutants M4B and KIX P/E showed no supershifting activity when added to phospho-Ser-133 CREB–CRE complexes (Fig. 3B, lanes marked M4B and KIX P/E), indi-

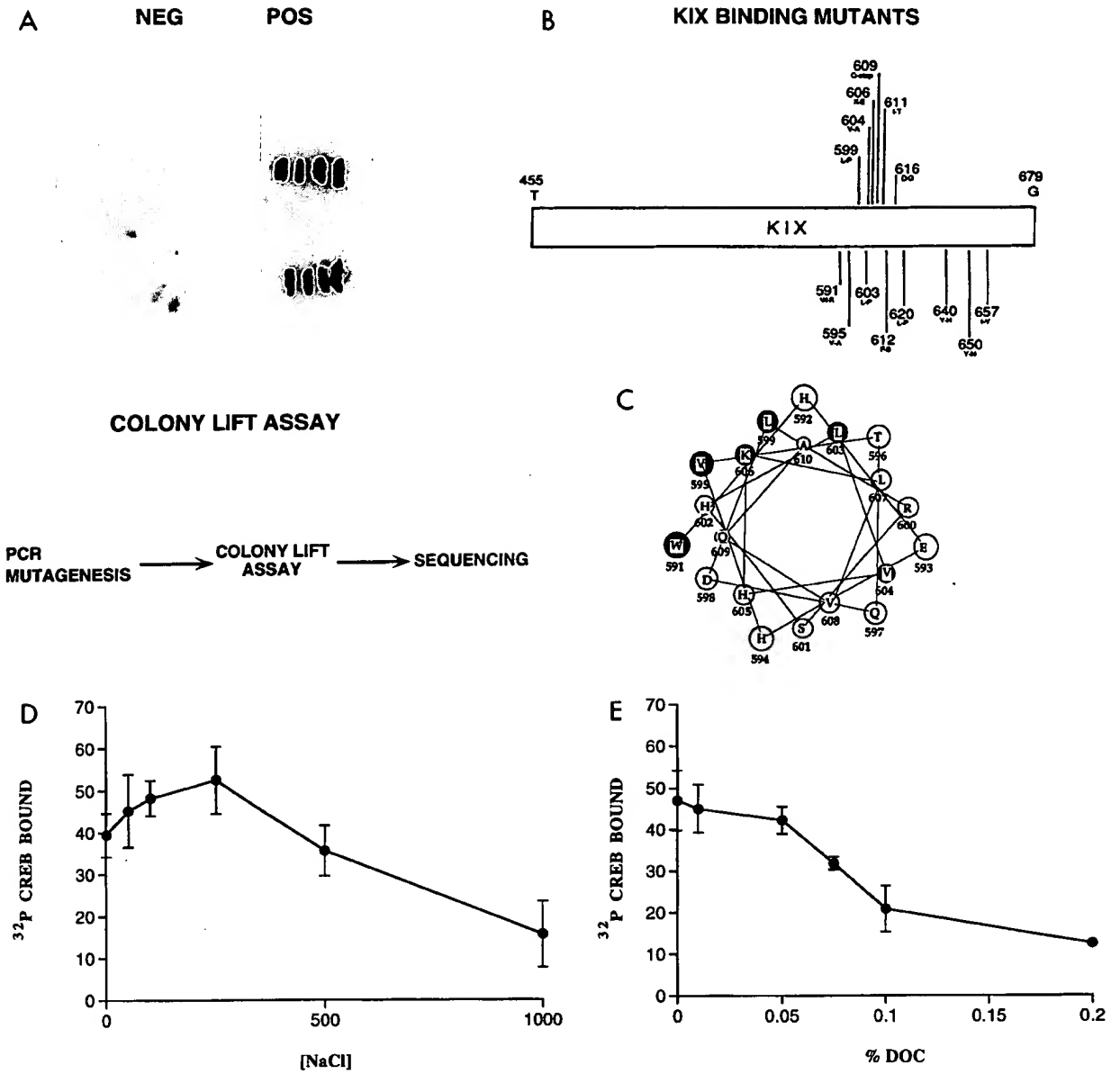


FIG. 2. Hydrophobic interactions contribute to CREB-CBP complex formation. (A) Colony lift assay used to detect mutant KIX (aa 455 to 679) cDNAs, generated by random PCR mutagenesis, which are deficient in phospho-Ser-133 CREB binding activity. Shown is an autoradiogram of nitrocellulose filters streaked with bacterial colonies expressing GST-KIX (POS) or an unrelated protein, GST–corticotropin releasing factor-binding protein (GST-CRF BP) (NEG). (B) Mutations in KIX polypeptides which are unable to bind $^{32}$P-labeled phospho-Ser-133 CREB. Amino acid substitutions are indicated in the single-letter code beneath the residue numbers. (C) Helical wheel map of KIX showing predicted positions of deleterious mutations (shaded in black). (D and E) Effect of NaCl and deoxycholate (DOC) on CREB-CBP interaction in vitro. (D) GST affinity chromatography of $^{32}$P-labeled phospho-Ser-133 CREB on GST-KIX (aa 455 to 679) resin. The percentage of CREB bound to the resin is expressed as a function of the NaCl concentration. (E) Effect of deoxycholate on $^{32}$P-CREB binding activity. (F) Pull-down assay of $^{32}$P-labeled wild-type (WT) and mutant {Ile-137–Leu-138→Ala-Ala [IL(137/8)AA]} phospho-Ser-133 KID peptides using wild-type GST-KIX S/B and mutant GST-KIX P/E polypeptides attached to glutathione-Sepharose beads. The arrows point to full-length KID peptides. The smaller peptide in each autoradiogram corresponds to the proteolytic product. ONPUT, labeled KID peptide applied to each resin.

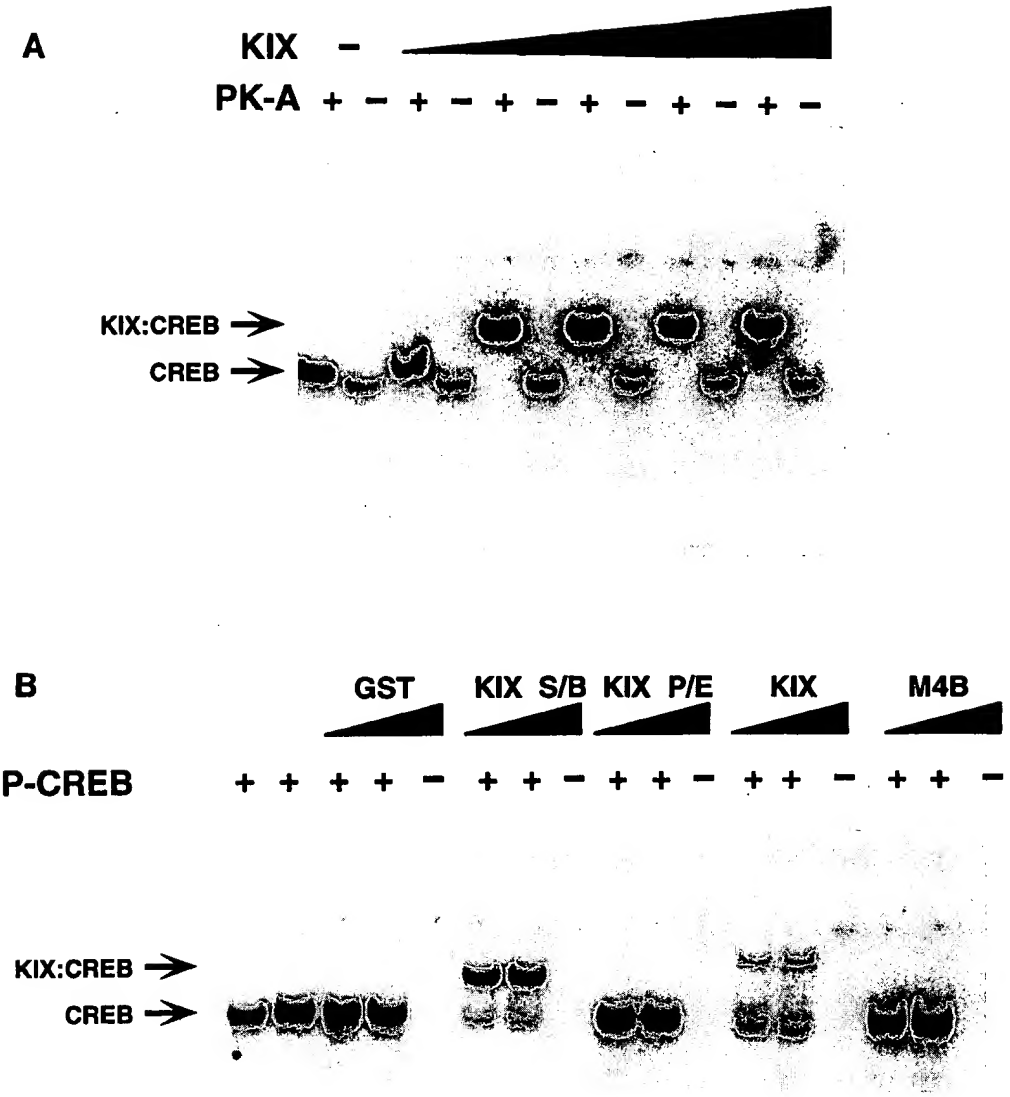


FIG. 3. The KIX polypeptide is recruited to cAMP-responsive promoters in a phospho-Ser-133 CREB-dependent manner and inhibits transcriptional induction by cAMP in vivo. (A and B) Gel shift assay with a somatostatin gene CRE double-stranded oligonucleotide and recombinant CREB protein. (A) Effect of increasing concentrations of KIX (indicated by crescendo bar). +, reaction mixture containing PKA catalytic subunit; −, reaction mixture lacking PKA catalytic subunit. CREB indicates the position of the CREB-CRE complex. KIX:CREB indicates the position of the KIX–phospho-Ser-133 CREB–CRE complex. (B) Gel shift assay of wild-type and mutant KIX polypeptides in the presence of phospho-CREB (P-CREB) (+) or no CREB (−). Crescendo bars indicate increasing amounts of protein in the gel shift assay. Arrows point to CREB-CRE (CREB) or KIX-CREB-CRE (KIX:CREB) complexes. GST, GST alone; KIX S/B, aa 553 to 679; KIX P/E, aa 455 to 679; KIX, aa 455 to 679; M4B, mutant KIX polypeptide (identified in PCR mutagenesis screen) which contains two deleterious point mutations (I-611→T and Y-650→N). (C to E) Microinjection of the KIX peptide inhibits cAMP-inducible transcription. Quiescent NIH 3T3 fibroblast nuclei were microinjected with the pCRE-β-galactosidase reporter plasmid, marker IgG, and either a mutant peptide, M4B (C), or the KIX peptide (D). The cells were stimulated with forskolin-IBMX for 2 h, fixed, and then assayed for β-galactosidase activity. Subsequently, the cells were permeabilized and immunostained with a secondary anti-rabbit antibody conjugated to fluorescein isothiocyanate to determine the number of cells that had been microinjected. The dark cells in panel C were all injected with the M4B peptide; the cells in panel D that were injected with KIX are indicated by arrows. (E) As a control, constitutive reporter activity was assessed in the presence of the KIX peptide. Cells were microinjected with pCMX-β-galactosidase, marker IgG, and the KIX peptide. All of the dark cells in panel E were microinjected, and no inhibition by the peptide was observed.

cating that the recruitment of KIX to such complexes occurs via a direct interaction with phospho-CREB.

The ability of KIX to be recruited to a cAMP-responsive promoter element prompted us to test whether KIX can inhibit cAMP-responsive transcription by competing for interaction between cellular CBP and CREB (Fig. 3C to E). NIH 3T3 fibroblasts were microinjected with the forskolin- and IBMX-inducible pCRE-β-galactosidase reporter construct along with either the KIX S/B polypeptide or the CREB binding mutant M4B polypeptide, which contains two inactivating point mutations (I-611→T and Y-650→N). Microinjection of the KIX S/B peptide inhibited reporter activity in response to the agonist (Fig. 3D), whereas the mutant KIX M4B peptide had no effect on pCRE-β-galactosidase activity (Fig. 3C). Of the 147 cells injected with the M4B peptide, 92.3% ± 3.9% (mean ± standard deviation) displayed cAMP-dependent transcription, as


FIG. 3—*Continued.*

determined by the number of blue cells, compared with only 0.5% ± 0.3% of the 415 cells that were microinjected with the KIX peptide. Microinjection of the KIX peptide had no effect on β-galactosidase activity derived from a constitutive cytomegalovirus promoter construct (Fig. 3E). In that case, 100% ± 0% of the 159 cells injected were blue. These data suggest that the ability of KIX to block cAMP-responsive transcription in vivo is consistent with its ability to associate with phospho-CREB in vitro.

**The PKA phosphoacceptor site in CREB participates directly in binding to CBP.** The relatively large region of CREB involved in binding to CBP (KID [aa 88 to 160]) prompted us to examine whether smaller CREB peptides might also bind to CBP in a phosphorylation-dependent manner. In this experiment, small phospho-Ser-133 CREB peptides could indeed bind to KIX, albeit with a lower affinity than full-length CREB. The dissociation constant ($K_d$) of phospho-Ser-133 $CREB_{121-151}$ for binding to KIX, for example, was 6.5 μM, compared with 32 nM for full-length phospho-Ser-133 CREB (Fig. 4). A 14-aa phospho-Ser-133 $CREB_{128-141}$ peptide recognized KIX with a $K_d$ of 0.56 mM, suggesting that sequences flanking the Ser-133 phosphoacceptor site stabilized complex formation. However, none of the unphosphorylated CREB peptides showed detectable binding to KIX (not shown), demonstrating that complex formation was phosphorylation dependent.

The ability of a 4-aa $CREB_{131-134}$ peptide to recognize KIX in a phospho-Ser-133-dependent manner (Fig. 4B), albeit with a low affinity, indicated that phospho-Ser-133 may participate directly in binding of CREB to CBP. However, free phosphoserine was unable to compete for binding of phospho-CREB to KIX in displacement assays (not shown), suggesting that the interaction of phosphoserine with KIX may be either weak or too unstable to detect by this method. To further test this model, we employed a phosphatase protection assay using the Ser/Thr protein phosphatases PP1 and PP2A, which have been shown to dephosphorylate CREB at Ser-133 in vitro and in vivo (Fig. 5). When added to $^{32}$P-labeled phospho-Ser-133 CREB, both phosphatases stimulated Ser-133 dephosphoryla-

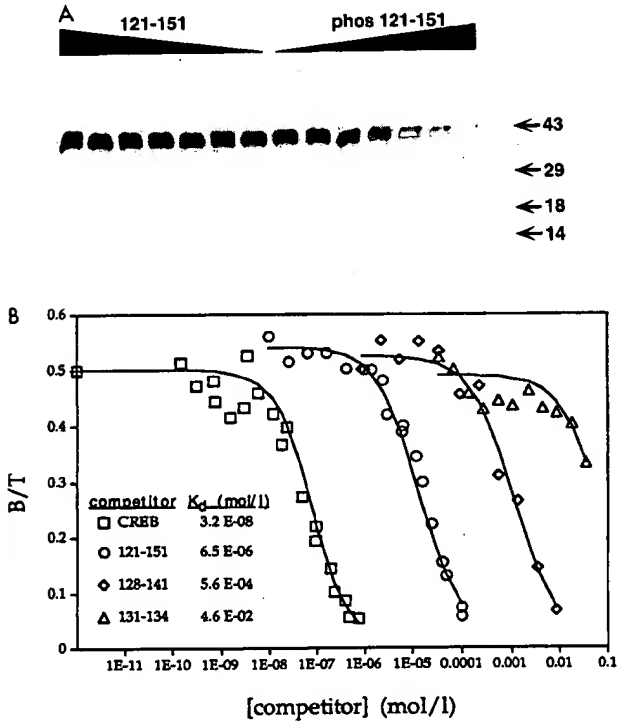


FIG. 4. Flanking residues in CREB stabilize phosphorylation-dependent interaction with KIX. (A) Typical autoradiogram showing results of a displacement assay with phosphorylated (phos 121-151) or unphosphorylated (121-151) $CREB_{121-151}$ peptide. The effect of increasing amounts of CREB peptide (indicated by crescendo bars) on binding of $^{32}$P-labeled phospho-Ser-133 CREB to KIX is shown. Molecular weights in thousands are indicated on the right. (B) Binding of $^{32}$P-phosphorylated CREB to GST-KIX S/B was measured in the presence of increasing concentrations of unlabeled phospho-CREB (CREB) or phospho-Ser-133 peptides representing the indicated amino acids of the KID. The displacement curves were analyzed by the LIGAND program, and the resulting best-fit curves are shown. The calculated $K_d$s for the various competitors are also given. B/T, bound/total (fraction of $^{32}$P-labeled CREB bound to KIX resin).

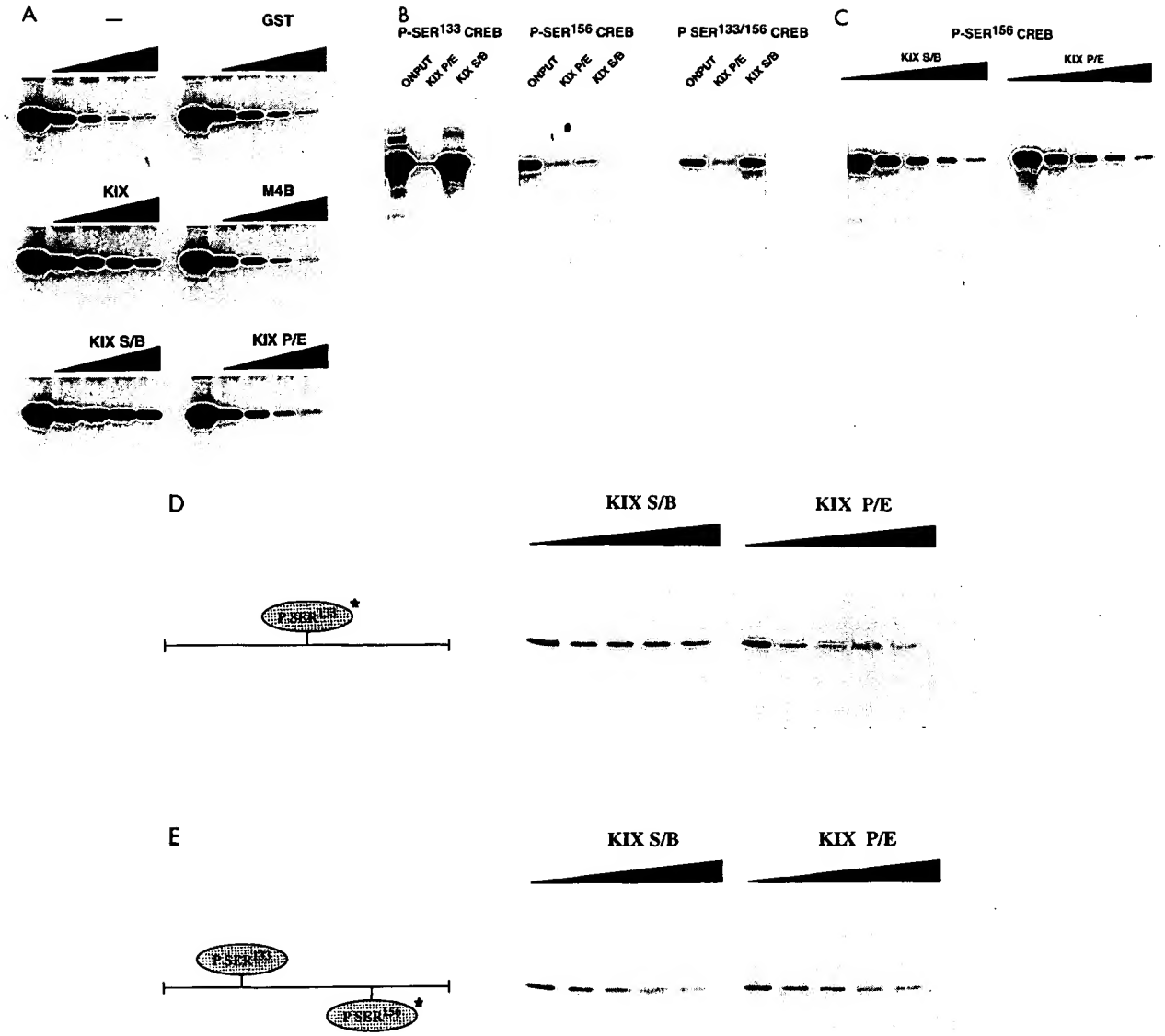


FIG. 5. The KIX domain forms unique contacts with the PKA phosphoacceptor Ser-133 in CREB. (A) Phosphatase protection assay with recombinant $^{32}$P-labeled CREB phosphorylated in vitro with PKA. Phospho-CREB was coincubated with the Ser/Thr protein phosphatase PP2A for increasing times (as indicated by crescendo bars) in the presence of various polypeptides indicated above the crescendo bars. Samples were then analyzed by SDS-PAGE. −, no added protein; GST, control; KIX, purified KIX polypeptide (aa 455 to 679); M4B, KIX mutant identified in PCR mutagenesis screen and containing two inactivating point mutations (I-611→T and Y-650→N); KIX S/B, aa 553 to 679; KIX P/E, aa 455 to 597. (B and C) The casein kinase II phosphoacceptor site in CREB (Ser-156) does not associate with CBP and is not protected from dephosphorylation by PP2A. (B) GST affinity chromatography of PKA-phosphorylated (P-SER$^{133}$ CREB), casein kinase II-phosphorylated (P-SER$^{156}$ CREB), or doubly phosphorylated (P SER$^{133/156}$ CREB) CREB. Lanes: ONPUT, total $^{32}$P-labeled CREB applied to KIX resins; KIX P/E and KIX S/B, CREB binding to GST-KIX P/E and GST-KIX S/B resins, respectively. The autoradiogram shows $^{32}$P-labeled CREB bound to each resin. (C) PP2A protection assay of Ser-156 phospho-CREB in the presence of the KIX S/B or KIX P/E polypeptide. Crescendo bars indicate increasing times of incubation (from 0 to 2 h) with PP2A. (D and E) Phospho-Ser-133 forms contacts with the KIX domain different from those formed by phospho-Ser-156. (D) PP2A-mediated dephosphorylation of CREB at Ser-133 in the presence of the wild-type KIX S/B or mutant KIX P/E polypeptide. (E) PP2A-mediated dephosphorylation at Ser-156 of doubly phosphorylated (at Ser-133 and Ser-156) CREB as indicated in the diagram on the left. CREB was phosphorylated at Ser-156 with casein kinase II. In panels D and E, asterisks denote sites phosphorylated with $^{32}$P-labeled ATP, and crescendo bars indicate increasing incubation times from left to right.

tion in a linear fashion over a 2-h period (Fig. 5A, panel −). When these phosphatases were coincubated with the KIX or KIX S/B polypeptide, however, CREB dephosphorylation by the phosphatases was markedly inhibited (Fig. 5A, panels KIX and KIX S/B). By contrast, mutant KIX polypeptides M4B and P/E, which do not bind phospho-Ser-133 CREB, had no effect on the rate of CREB dephosphorylation (Fig. 5A, panels M4B and KIX P/E), suggesting that KIX may form unique contacts with phospho-Ser-133, perhaps in the form of a pocket.

To test whether other residues in the KID interact similarly with KIX, we prepared $^{32}$P-labeled CREB phosphorylated at Ser-156 by casein kinase II. Phospho-Ser-156 CREB did not bind to GST-KIX in pull-down assays (Fig. 5B; compare lanes 3 in panels P-SER$^{133}$ CREB and P-SER$^{156}$ CREB), and cor-

respondingly, the KIX polypeptide could not protect CREB from PP2A-mediated dephosphorylation at Ser-156 (Fig. 5C). Upon phosphorylation with PKA using unlabeled ATP, the doubly phosphorylated phospho-Ser-133/phospho-Ser-156 CREB protein showed a wild-type level of binding to GST-KIX resins (Fig. 5B, panel P $SER^{133/156}$ CREB, lane 3). But KIX did not protect the doubly phosphorylated CREB from dephosphorylation at Ser-156 (Fig. 5D and E), demonstrating that phospho-Ser-133 forms specific contacts with residues in KIX.

To further investigate whether phospho-Ser-133 directly participates in binding to CBP, we performed cross-linking assays using platinum tetrachloride, a reagent with high affinity for sulfhydryl groups (5) (Fig. 6A). The absence of sulfur-containing residues in the $CREB_{121-151}$ peptide prompted us to construct a platinum adduct with this peptide following its thiophosphorylation at Ser-133 with $\gamma$-$^{35}$S-ATP. In solution binding assays, phosphorylated and thiophosphorylated $CREB_{121-151}$ peptides bound with comparable affinities to KIX (not shown). When incubated with the purified KIX peptide (14.3 kDa) in the presence of platinum tetrachloride, the $^{35}$S-labeled 3.6-kDa $CREB_{121-151}$ thiophosphorylated peptide gave rise to an 18-kDa cross-linked product (Fig. 6A, lane 4) whose size is consistent with the predicted molecular mass for the thiophospho-Ser-133 $KID_{121-151}$–KIX complex. No cross-linked complex was detected in samples in which the $^{35}$S-labeled CREB peptide was incubated with nonspecific proteins such as BSA or with the phospho-CREB-binding mutant peptide KIX P/E (not shown). To determine whether platinum-dependent cross-linking of $CREB_{121-151}$ to KIX occurred via the thiophosphate moiety at Ser-133 or via other residues in the peptide, we prepared $^{32}$P-labeled phospho-Ser-133 $CREB_{121-151}$, which contained only a phosphate moiety at Ser-133. When incubated with the KIX polypeptide in the presence of platinum, phospho-Ser-133 $CREB_{121-151}$ did not form any covalent complexes (Fig. 6A, lane 6), demonstrating that thiophosphorylation at Ser-133 is essential for platinum-dependent cross-linking. The short bond distance for platinum (2 Å [0.2 nm]) compared with those of other cross-linking reagents indicates that phospho-Ser-133 is positioned next to residues in KIX which are important for complex formation.

To identify residues in KIX which interacted with the thiophosphorylated Ser-133, we subjected the platinum-cross-linked $CREB_{121-151}$–KIX complex to trypsin proteolysis. Following their resolution by reverse-phase high-performance liquid chromatography (HPLC), individual tryptic peptides were evaluated for the presence of cross-linked $^{35}$S-labeled phospho-Ser-133 by scintillation counting (Fig. 6B). We identified one $^{35}$S-labeled peptide which contained two peptide sequences: SHLVXK, corresponding to aa 601 to 606 (SHLVHK) in CBP, and XPXY, corresponding to aa 131 to 134 (RPSY) in CREB. In the process of examining sequences surrounding the KIX tryptic peptide (aa 601 to 606), we noticed an adjacent arginine residue (Arg-600) which was conserved in P300 and in the *C. elegans* homolog R10e11.1. The unique capacity of arginine residues to form ion pairs with phosphorylated amino acids prompted us to examine whether Arg-600 was important for phospho-CREB recognition. Mutagenesis of Arg-600 to Gln severely disrupted complex formation with phospho-Ser-133 CREB in far Western blotting and solution binding assays (Fig. 6C, fractions 7 to 9). These results indicate that Arg-600 is indeed critical for phosphoserine recognition.

## DISCUSSION

Serine phosphorylation has been shown to regulate protein activity by at least two different mechanisms: direct and allosteric. For example, phosphorylation of glycogen phosphorylase at Ser-14 augments catalytic activity via an allosteric mechanism which involves altered subunit interactions (16). By contrast, phosphorylation of isocitrate dehydrogenase at Ser-113 causes few changes in its tertiary structure (10). Ser-113 is located within the active site of isocitrate dehydrogenase, and phosphorylation there inhibits enzyme-substrate interactions by electrostatic repulsion.

Previous experiments with CREB had prompted us to speculate that phosphorylation might regulate this protein via an allosteric mechanism. This model was supported by mutagenesis data showing that acidic residues could not substitute for Ser-133 (7). Moreover, the presence of a constitutive activation domain in CREB termed Q2 (aa 161 to 283), which is removed from the PKA site, suggested that phosphorylation might regulate CREB by exposing this domain to the transcriptional apparatus. More recent experiments have revealed that the KID and Q2 can synergize not only in *cis* but also in *trans* in response to PKA induction (2), providing strong evidence against this allosteric model. In this study, circular dichroism and one-dimensional nuclear magnetic resonance analyses revealed that the KID assumes a disordered structure which is unaffected by Ser-133 phosphorylation.

Ser-133 phosphorylation appears to promote interaction with CBP via a direct mechanism. In this regard, phosphatase protection assays revealed that KIX interacts uniquely with phospho-Ser-133 upon binding to the KID. Indeed, a small 4-aa CREB peptide (aa 131 to 134) interacts with CREB in a phosphorylation-dependent manner, suggesting that phospho-Ser-133 drives the specificity of the interaction with CBP. This hypothesis was substantiated by platinum cross-linking experiments in which phospho-Ser-133 itself was found to come into close contact with residues 601 to 606 in the KIX polypeptide. Although we could not identify the specific amino acid which coordinates with platinum in these cross-linking experiments, the high affinity of platinum for imidazole rings implicates histidines 602 and 606 in this process. Indeed, the presence of a conserved arginine (Arg-600) which lies adjacent to the cross-linked tryptic KIX peptide and which is required for complex formation suggests that this residue may coordinate with phosphoserine 133 in CREB.

KIX has a number of interesting similarities to the phosphotyrosine binding src homology 2 (SH2) domain (15). The minimal KIX domain (KIX 10.4 [aa 586 to 679]) is similar in size to the SH2 motif (100 aa), and, like SH2 domains, it appears to recognize an unstructured region of CREB by binding directly to the phosphorylated amino acid (Ser-133). As with SH2 domains, high-affinity interaction between KIX and phospho-CREB requires residues which flank the Ser-133 phosphoacceptor site. These flanking residues may stabilize complex formation primarily via hydrophobic interactions. Ile-137 and Leu-138 in CREB, for example, were found to contribute importantly to high-affinity interaction with the KIX domain. Moreover, complex formation between KIX and phospho-Ser-133 CREB was found to be stable in the presence of high concentrations of KCl but susceptible to low levels of nonionic detergent.

How, then, does CBP recognize phospho-Ser-133 CREB? Structural studies reveal that, in contrast to the SH2 motif, KIX is highly helical. In particular, one segment of KIX (aa 590 to 610) may adopt an amphipathic helical form which is critical for complex formation. Indeed, the majority of phos-

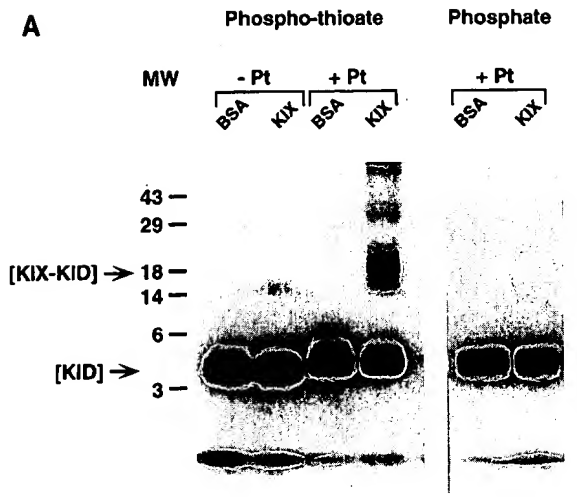


FIG. 6. Phospho-Ser-133 in CREB interacts directly with residues in CBP. (A) Cross-linking assay with $CREB_{121-151}$ and KIX S/B peptides. Phosphothioate, thiophosphorylated $CREB_{121-151}$ labeled at Ser-133 with PKA by using $\gamma^{35}$S-ATP; Phosphate, phosphorylated $CREB_{121-151}$ labeled at Ser-133 with PKA by using [$\gamma$-$^{32}$P]ATP. The absence (− Pt) or presence (+ Pt) of platinum tetrachloride in binding reactions is indicated. MW, relative molecular weight in thousands. The phospho-$CREB_{121-151}$ peptide was incubated with BSA as a control or KIX peptide as indicated above each lane. The arrows point to the labeled phospho-$CREB_{121-151}$ peptide (KID) and the cross-linked KID-KIX complex (KIX-KID). (B) Reverse-phase HPLC analysis of peptides generated after trypsinization of the platinum-cross-linked KIX–$^{35}$S-phospho-KID complex. The dashed line indicates the ascending gradient of acetonitrile. The primary sequences derived after automated Edman degradation of peptides in peak 21 are indicated. SHLVXL corresponds to aa 601 to 606 of CBP, and XPXY corresponds to aa 131 to 134 of CREB. (C) Analysis of peptide fractions obtained from HPLC (B). The $^{35}$S counts per minute correspond to $^{35}$S-labeled thiophospho-Ser-133. (D and E) Arg-600 in KIX is critical for complex formation with phospho-Ser-133 CREB. (D) Western blot (immunoblot) assay of GST-KIX (WT-KIX), GST-KIX P/E, and GST-R600Q proteins with anti-CBP antiserum raised against the KIX S/B polypeptide. KIX P/E does not react with anti-CBP antiserum. (E) Far Western blot assay of wild-type and mutant KIX proteins with $^{32}$P-labeled phospho-Ser-133 CREB as a probe. In panels D and E, crescendo bars indicate increasing amounts of purified recombinant proteins. MW, relative molecular weight in thousands.

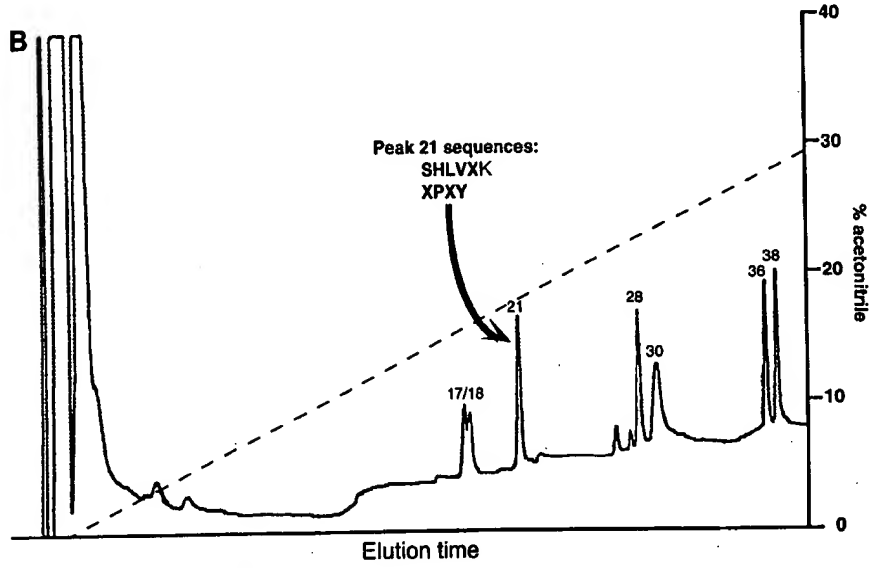


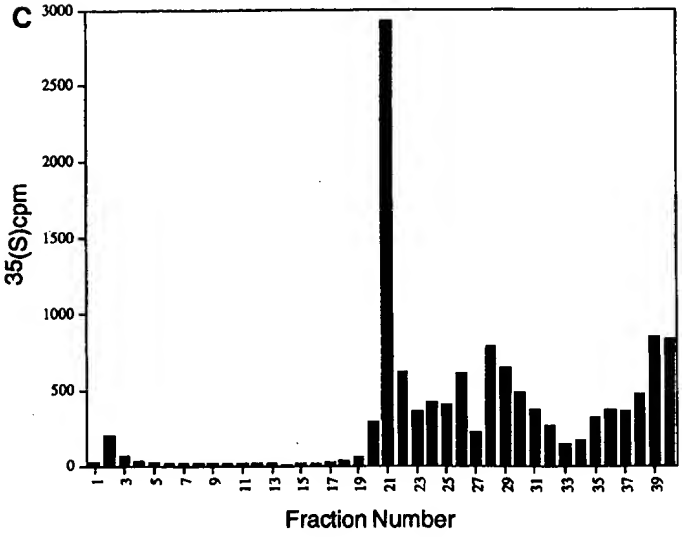


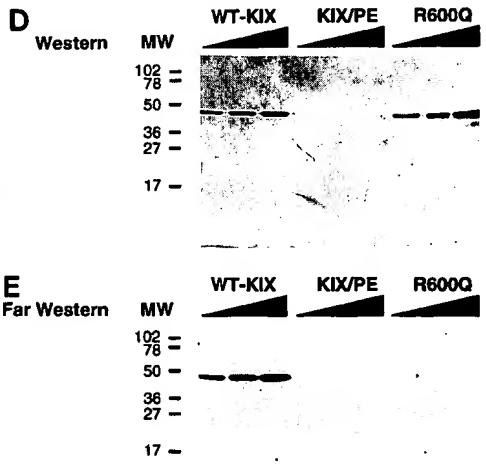

pho-Ser-133 CREB binding mutants obtained from a random mutagenesis screen of KIX were targeted to hydrophobic residues within this amphipathic helix. These amino acids appear to cluster on a helical face opposite Arg-600, which we propose here to coordinate with phospho-Ser-133 in CREB. Thus, hydrophobic residues in the amphipathic helix (aa 590 to 610) may be more important for proper folding of the KIX domain than for direct interaction with hydrophobic residues in CREB.

The functional importance of CBP in cAMP-responsive transcription has been previously demonstrated by microinjection experiments in which anti-CBP antiserum abrogated the response to an agonist (1) and by transient-transfection assays in which overexpression of CBP potentiated CREB activity in a Ser-133-dependent manner (11). Our results reveal that CBP is recruited to cAMP-responsive elements upon phosphorylation of CREB. Furthermore, microinjection experiments with the KIX peptide demonstrate that this recruitment is critical for target gene induction in response to cAMP. Other growth factor pathways, such as those induced by the transforming growth factor β family, stimulate target cell responses via receptor Ser/Thr kinases (13). The intracellular events which follow transforming growth factor β induction remain to be elucidated, but it is tempting to speculate that, like the tyrosine kinase-linked receptors, these Ser/Thr kinase receptors may also induce protein-protein interactions via motifs which resemble the KIX domain.

## ACKNOWLEDGMENTS

We thank Leslie Orgel and B. Chu for suggesting platinum crosslinking experiments. We also thank T. Hunter for a critical review of the manuscript, members of the laboratory of Marc Montminy for helpful discussions, and H. Do for expert technical assistance.

This work was supported in part by the Foundation for Medical Research, Inc., and by NIH grants CA54418 and GM37828.

The first two authors contributed equally to this work.

## REFERENCES

1. **Arias, J., A. Alberts, P. Brindle, F. Claret, T. Smeal, M. Karin, J. Feramisco, and M. Montminy.** 1994. Activation of cAMP and mitogen responsive genes relies on a common nuclear factor. Nature (London) **370**:226–228.
2. **Brindle, P., S. Linke, and M. Montminy.** 1993. Analysis of a PK-A dependent activator in CREB reveals a new role for the CREM family of repressors. Nature (London) **364**:821–824.
3. **Chang, C. T., S. Wu, and J. Yang.** 1978. Circular dichroic analysis of protein conformation: inclusion of the β-turns. Anal. Biochem. **92**:13–31.
4. **Chrivia, J. C., R. P. Kwok, N. Lamb, M. Hagiwara, M. R. Montminy, and R. H. Goodman.** 1993. Phosphorylated CREB binds specifically to the nuclear protein CBP. Nature (London) **365**:855–859.
5. **Chu, B., and L. Orgel.** 1992. Crosslinking transcription factors to their recognition sequences with $Pt^{II}$ complexes. Nucleic Acids Res. **20**:2497–2502.
6. **Eckner, R., M. E. Ewen, D. Newsome, M. Gerdes, J. A. DeCaprio, J. B. Lawrence, and D. M. Livingston.** 1994. Molecular cloning and functional analysis of the adenovirus E1A-associated 300-kD protein (p300) reveals a protein with properties of a transcriptional adaptor. Genes Dev. **8**:869–884.
7. **Gonzalez, G. A., and M. R. Montminy.** 1989. Cyclic AMP stimulates somatostatin gene transcription by phosphorylation of CREB at serine 133. Cell **59**:675–680.
8. **Hagiwara, M., P. Brindle, A. Harootunian, R. Armstrong, J. Rivier, W. Vale, R. Tsien, and M. R. Montminy.** 1993. Coupling of hormonal stimulation and transcription via the cyclic AMP-responsive factor CREB is rate limited by nuclear entry of protein kinase A. Mol. Cell. Biol. **13**:4852–4859.
9. **Hunter, T., and M. Karin.** 1992. The regulation of transcription by phosphorylation. Cell **70**:375–387.
10. **Hurley, J., A. Dean, J. Sohl, D. Koshland, and R. Stroud.** 1990. Regulation of an enzyme by phosphorylation at the active site. Science **249**:1012–1016.
11. **Kwok, R. P., J. R. Lundblad, J. C. Chrivia, J. P. Richards, H. Bachinger, R. Brennan, S. Roberts, M. Green, and R. H. Goodman.** 1994. Nuclear protein CBP is a coactivator for the transcription factor CREB. Nature (London) **370**:223–226.
12. **Leung, D. W., E. Chen, and D. Goeddel.** 1989. A method for random mutagenesis of a defined DNA segment using a modified polymerase chain reaction. Technique **1**:11–15.
13. **Mathews, L., and W. Vale.** 1991. Expression cloning of an activin receptor, a predicted transmembrane serine kinase. Cell **65**:973–982.
14. **Meinkoth, J., A. Alberts, and J. Feramisco.** 1990. Generation of mammalian cell lines with indicator genes driven by regulated promoters. Ciba Found. Symp. **150**:47–56.

14a. **Montminy, M., I. Radhakrishnan, and P. Wright.** Unpublished data.

15. **Pawson, T., and G. Gish.** 1992. SH2 and SH3 domains: from structure to function. Cell **71**:359–362.
16. **Sprang, S. R., K. R. Acharya, E. J. Goldsmith, D. I. Stuart, K. Varvill, R. J. Flettrick, N. B. Madsen, and L. N. Johnson.** 1988. Structural changes in glycogen phosphorylase induced by phosphorylation. Nature (London) **336**: 215–221.

# A functional R domain from cystic fibrosis transmembrane conductance regulator is predominantly unstructured in solution

**Lynda S. Ostedgaard*, Olafur Baldursson*, Daniel W. Vermeer*, Michael J. Welsh*†‡§, and Andrew D. Robertson¶**

†Howard Hughes Medical Institute, *Departments of Internal Medicine, §Physiology and Biophysics, and ¶Biochemistry, University of Iowa College of Medicine, Iowa City, IA 52242

Edited by Lily Y. Jan, University of California, San Francisco, CA, and approved March 7, 2000 (received for review January 3, 2000)

**Phosphorylation of the regulatory (R) domain initiates cystic fibrosis transmembrane conductance regulator (CFTR) $Cl^-$ channel activity. To discover how the function of this domain is determined by its structure, we produced an R domain protein (R8) that spanned residues 708–831 of CFTR. Phosphorylated, but not unphosphorylated, R8 stimulated activity of CFTR channels lacking this domain, indicating that R8 is functional. Unexpectedly, this functional R8 was predominantly random coil, as revealed by CD and limited proteolysis. The CD spectra of both phosphorylated and nonphosphorylated R8 were similar in aqueous buffer. The folding agent trimethylamine *N*-oxide induced only a small increase in the helical content of nonphosphorylated R8 and even less change in the helical content of phosphorylated R8. These data, indicating that the R domain is predominantly random coil, may explain the seemingly complex way in which phosphorylation regulates CFTR channel activity.**

Cystic fibrosis (CF) transmembrane conductance regulator (CFTR) is a phosphorylation-regulated $Cl^-$ channel that provides a pathway for $Cl^-$ movement across epithelial membranes in the airways, sweat gland, intestine, and pancreas (1, 2). Loss of CFTR function causes the genetic disease CF. CFTR $Cl^-$ channel activity is regulated by cAMP-dependent protein kinase (PKA) and protein kinase C phosphorylation of the regulatory (R) domain (3–8). After phosphorylation of the R domain, ATP binding and hydrolysis by the two nucleotide-binding domains (NBDs) gate the channel (7, 8).

The R domain has a unique primary sequence with no homology to any known protein (1). The R domain was originally defined as those residues encoded by exon 13 (residues 590–830) (1). However, the N-terminal half of exon 13 shares sequence similarity with the NBDs of other ATP-binding cassette (ABC) transporters (9, 10). Compelling evidence that the N-terminal portion of exon 13 is actually part of NBD1 came from the crystal structure of HisP, the NBD of the histidine permease ABC transporter (11). In CFTR, an NBD structure analogous to that of HisP would extend to approximately residue 660. The C-terminal half of exon 13 appears to be the functional R "regulatory" domain (9, 10). Consistent with this, deletion of residues 708–835 produces a CFTR channel with properties like those of wild-type CFTR, suggesting that residues 708–835 form a functional R domain that can be deleted (9, 12–14). More extensive deletions (residues 590–835, 656–835, 676–835, or 681–835) disrupted function (9), probably because they disrupt a portion of NBD1.

Exon 13 contains eight serines in consensus motifs for PKA phosphorylation; five of these serines, S660, S700, S737, S795, and S813, are phosphorylated in cells (15–17). The contribution of the various phosphoserines to channel activity is complex. No one serine is required for activity; mutation of single or multiple serines decreases, but does not abolish, phosphorylation-stimulated activity (6, 13, 15, 18–21). Phosphorylation of several different serines can stimulate channel activity, although not all of the serines have the same quantitative effect on channel activity. Mutating the consensus serines to aspartate, to mimic the negative charge imposed by phosphorylation, stimulated channel activity in the absence of phosphorylation (19), suggesting that negative charge plays a role in channel stimulation. Earlier work suggested that phosphorylation of the R domain stimulates channel activity by increasing the binding and/or hydrolysis of ATP by the NBDs (13, 22).

Additional clues to the mechanism by which the R domain regulates channel activity came from studies in which parts of the R domain were deleted and/or synthesized as separate proteins and then added back to the channel. An example is CFTR-ΔR/S660A, in which residues 708–835 are deleted and Ser-660 is mutated to alanine (12, 19, 23). CFTR-ΔR/S660A lacks the serines (660, 737, 795, and 813) shown to be responsible for the majority of PKA-stimulated channel activity (6, 15, 16, 19). This channel differs from wild-type CFTR in two important ways: it has a low level of constitutive $Cl^-$ channel activity in the absence of PKA-dependent phosphorylation, and its activity is not altered by addition of PKA (9, 12–14).

Constitutive activity of CFTR-ΔR/S660A suggests that the unphosphorylated R domain might have an inhibitory function (12). In support of this idea, application of an unphosphorylated R domain protein (residues 588–855) to wild-type CFTR in lipid bilayers was reported to inhibit activity (23). However, another study observed no effect of the unphosphorylated R domain protein R1 (residues 645–834) on wild-type CFTR channels in excised cell-free patches of membranes (13). Moreover, neither unphosphorylated R1 nor the unphosphorylated 588–855 protein had an effect on CFTR-ΔR/S660A (13, 14). Furthermore, if the function of the R domain were primarily inhibitory, the activity of CFTR-ΔR/S660A would be expected to be equal to or greater than that of the phosphorylated wild-type channels. In contrast to this prediction, the activity of CFTR-ΔR/S660A is approximately one-third that of phosphorylated wild-type CFTR (13, 19). Thus whether the R domain has an inhibitory role remains uncertain.

Other evidence indicates that the phosphorylated R domain has a stimulatory role. Recombinant protein containing residues 645–835 stimulated CFTR-ΔR/S660A activity in excised membrane patches and residues 588–855 stimulated CFTR-ΔR/

PHYSIOLOGY

This paper was submitted directly (Track II) to the PNAS office.

Abbreviations: CFTR, cystic fibrosis transmembrane conductance regulator; CF, cystic fibrosis; R domain, regulatory domain; NBD, nucleotide-binding domain; PKA, cAMP-dependent protein kinase; NMDG, *N*-methyl-D-glucamine; TMAO, trimethylamine oxide; KID, kinase-inducible domain.

‡To whom reprint requests should be addressed at: Howard Hughes Medical Institute, University of Iowa College of Medicine, 500 EMRB, Iowa City, IA 52242. E-mail: mjwelsh@blue.weeg.uiowa.edu.

The publication costs of this article were defrayed in part by page charge payment. This article must therefore be hereby marked "*advertisement*" in accordance with 18 U.S.C. §1734 solely to indicate this fact.

Article published online before print: *Proc. Natl. Acad. Sci. USA*, 10.1073/pnas.100588797. Article and publication date are at www.pnas.org/cgi/doi/10.1073/pnas.100588797

S660A in lipid bilayers (13, 14). Phosphorylation was required for channel activation; the unphosphorylated R domain had no stimulatory effect.

All these data suggest that the R domain forms a unique structural and functional domain with boundaries from about residue 708 to approximately residue 830. The goal of this work was to determine the structure of an R domain construct comprising residues 708–831 (R8), which closely complements the deletion in CFTR-ΔR/S660A. We were encouraged by the finding that R8 retains stimulatory activity, suggesting that if the R domain has a specific structure, it is retained in this protein.

## Experimental Procedures

**Site-Directed Mutagenesis and Plasmids.** We amplified the R domain of wild-type CFTR and ligated the resultant fragment into the pET21d vector (Novagen). Vector splice sites and the insert coding sequence were verified by sequencing (University of Iowa DNA Core Facility). The amino acid sequence of R8 is MG-CFTR residues 708–831-LEHHHHHH.

**Bacterial Expression and Purification.** pET plasmids and pDC952 (encoding arginine tRNA) (a gift of James Walker, University of Texas, Austin, TX) were cotransformed into BL21 (DE3) (Novagen) on LB plus carbenicillin/chloramphenicol plates. We used the parental BL21 (DE3) cell line and not the derivative BL21 (DE3) pLysS, because the pLysS cells, but not the parental cells, produce sufficient levels of chloramphenicol acetyltransferase to interfere with subsequent purification of R8. Cultures were grown at 37°C to 0.6 OD at 600 nm, induced with 0.1 mM isopropyl-D-thiogalactoside, and grown for 3 h at 37°C. Cells were centrifuged at 3,500 × *g*, resuspended in binding buffer (BB) (20 mM Tris·HCl, pH 7.9/0.5 M NaCl/1 mM imidazole) and sonicated. After sonication, inclusion bodies were isolated by centrifugation at 39,000 × *g* for 20 min. The inclusion bodies were resuspended in BB with 6 M urea, solubilized overnight at 4°C, and centrifuged at 39,000 × *g* for 20 min to separate the urea-soluble and urea-insoluble pellet.

Proteins in the urea-soluble fraction were bound to Talon cobalt columns (CLONTECH) in BB and purified by using a step gradient of imidazole (10 mM to 500 mM) in BB. Protein concentrations were determined by the Bradford assay (Bio-Rad).

**Identification of R8.** R8 was analyzed by SDS/PAGE under nonreducing conditions. The composition of R8 was confirmed by amino acid analysis, sequencing of proteolytic fragments, and reactivity with the anti-CFTR antibody 13–1 (Genzyme).

**Phosphorylation of R8.** Purified protein was phosphorylated with 40 nM PKA/1 mM MgATP/3 mM $MgCl_2$ in 10 mM potassium phosphate ($KP_i$), pH 6.8, at 30°C.

**Proteolysis of R8.** R8 dialyzed into Hepes/NMDG-Cl buffer [in mM: 140 *N*-methyl-D-glucamine (NMDG), 3 $MgCl_2$/1 CsEGTA/10 Hepes (pH 7.3 with HCl; $Cl^-$ concentration, 140 mM)] was incubated at room temperature for the indicated time with either trypsin or papain (sequencing grade; Boehringer-Mannheim) (1:100, w:w, protease:R8). At each time point, 1 volume of ×2 sample buffer (62.5 mM Tris, pH 6.8/4% SDS/100 mM DTT/20% glycerol/0.005% bromophenol blue) was added to an aliquot of the reaction and boiled immediately for at least 3 min to inactivate proteases (24). For some experiments, 1 mM PMSF was added before sample buffer. Results did not differ with or without PMSF. After completion of the last time point, samples were electrophoresed on SDS/PAGE and stained with Coomassie blue. For sequencing, proteolytic fragments of R8 were quantitatively transferred to ProBlot nitrocellulose (IBI) (25) and sequenced by Edman degradation.

**Patch-Clamp Analysis.** We expressed CFTR-ΔR/S660A in HeLa cells by using the vaccinia virus/T7 hybrid expression system (19). Methods for excised inside-out patches were as previously described at 37°C and −40 mV (13). Pipette solution contained (in mM): 140 NMDG/2 $MgCl_2$/5 $CaCl_2$/100 L-aspartic acid/10 Hepes (pH 7.3 with HCl; $Cl^-$ concentration, 50 mM). Bath solutions were: Hepes/NMDG-Cl buffer or 10 $KP_i$, pH 7.3, with 100 NaCl. Similar results were obtained with both solutions. PKA (75 nM) and 1 mM ATP were present throughout patch recording. Data points are mean current during successive 10-s intervals.

**Analytical Ultracentrifugation.** Sedimentation equilibrium was conducted at 25°C on a Beckman XL-I ultracentrifuge (Beckman Coulter) equipped with an An-60 Ti rotor. Concentrations of R8 were 40, 20, and 10 μM in 10 mM glycine and 0.1 M NaCl, pH 9.0, similar to conditions used for some CD studies.

Samples were centrifuged at 17,000, 24,000, and 35,000 rpm. Absorbance was monitored at 236 nm. Data were analyzed by using ORIGIN software (Ver. 3.78, Microcal Software, Northampton, MA). The partial specific volume, $\bar{\nu}$, of R8 was calculated to be 0.711 ml/g on the basis of amino acid composition (26). The calculated solution density, $\rho$, for the samples was 1.004 g/ml (27). The apparent molecular weight of R8, M, was determined by the equation for an ideal solution containing a single species (28):

$$A(r) = A(r_0)\exp[M(1 - \nu\rho)\omega^2(r^2 - r_0^2)/2RT] + A_0. \quad [1]$$

**CD Analysis.** CD spectra were recorded on an Aviv CD Model 62DS (Aviv Associates, Lakewood, NJ) in an 0.2-cm pathlength quartz cuvette (Hellma, Forest Hills, NY) thermostated at 22°C. Spectra were collected from 260 to 210 nm at a bandwidth of 1 nm every 0.25 nm with a 2-s averaging time. Each spectrum is the result of three summed spectra corrected for solute buffer.

R8 was phosphorylated as described above in 1 mM glycine, pH 9.0, with 1 mM ATP, dialyzed to remove ATP and $MgCl_2$, and centrifuged at 200,000 × *g*. Parallel incubations and dialyses were carried out in the absence of PKA for nonphosphorylated R8. Spectra were obtained from nonphosphorylated and phosphorylated R8 diluted in the following buffers: (*i*) 1 mM glycine, pH 9; (*ii*) 10 mM $KP_i$, pH 7.3; or (*iii*) 10 mM $KP_i$, 100 mM NaCl, pH 7.3. Similar CD spectra were obtained with each buffer. The inclusion of 5 mM $MgCl_2$ or $MnCl_2$ had no effect on the spectrum. To analyze the effect of lipid, R8 was incorporated into a sonicated phospholipid mixture (PC/PS, 3:1).

For CD spectra in trimethylamine oxide (TMAO), concentrated R8 dialyzed into 1 mM glycine was diluted to 0.15 mg/ml in 10 mM $KP_i$, pH 7.3, or into 2.8 M recrystallized TMAO. Titration curves with TMAO were carried out at 220 nm, the wavelength of greatest difference between the R8 spectra in $KP_i$ and TMAO.

## Results

**Expression and Purification of R8.** We expressed and purified R8 by using the pET vector system and metal-affinity chromatography. To alleviate the problem of poor expression and protein truncation caused by the infrequent usage of the arginine codons AGA and AGG by *Escherichia coli*, we coexpressed R8 with the tRNA synthase for the AGA codon (29). R8 contains no cysteines, thus preventing dimerization and aggregation of the purified protein in the absence of reducing agents. We partially purified R8, which was sequestered in inclusion bodies, by isolating the inclusion body pellet (Fig. 1). After solubilization of the inclusion bodies in urea (lane 4), R8 was purified by metal-affinity chromatography (lanes 6–8). Typical 500-ml cultures yielded ≥10 mg R8 that was 94–97% pure.

After affinity purification, we dialyzed R8 to remove urea and

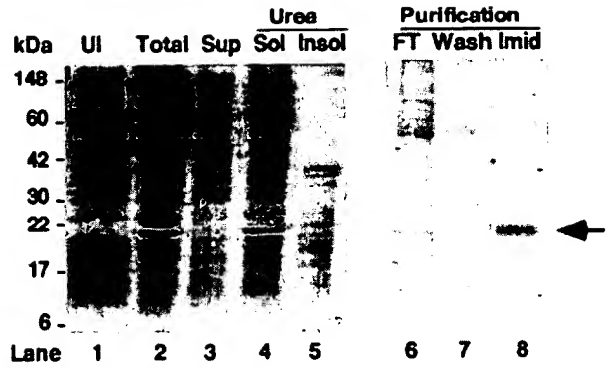


Fig. 1. Purification of R8. Coomassie-stained gel. Lane 1 (UI): before induction by IPTG. Lane 2 (Total): 3 h after IPTG. Lane 3 (Sup): supernatant from induced culture. Lane 4 (Urea Sol): urea-soluble fraction from inclusion bodies. Lane 5 (Urea Insol): urea-insoluble pellet. Lane 6 (FT): flow through from metal-affinity column. Lane 7 (Wash): wash with 1 mM imidazole. Lane 8 (Imid): elution with 200 mM imidazole. Arrow indicates R8.

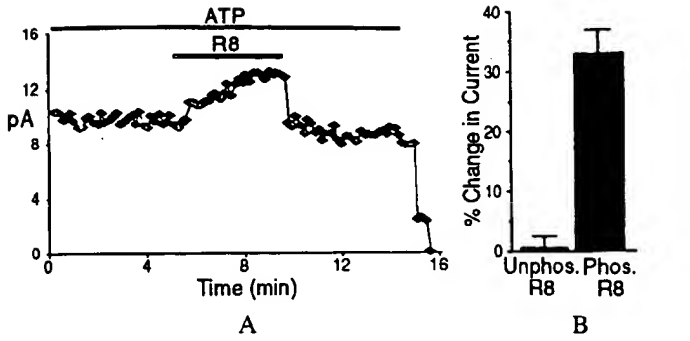


Fig. 3. R8 stimulation of CFTR-ΔR/S660A $Cl^-$ channel activity. (*A*) Current from excised inside-out patch containing many channels. Bars indicate exposure to ATP (1 mM) and phosphorylated R8 (1.5 μM). PKA (75 nM) was present throughout. (*B*) Change in current produced by unphosphorylated ($n$ = 4) and phosphorylated R8 ($n$ = 9).

imidazole and to promote protein folding. R8 was soluble (3–4 mg/ml) in 1 mM glycine or 10 mM Tris at pH 9 and (5–6 mg/ml) in Hepes/NMDG-Cl buffer (pH 7.3).

**Functional Studies of R8.** R8 was phosphorylated by PKA *in vitro* as indicated by the shift in electrophoretic migration of R8 on SDS/PAGE (Fig. 2). This shift is similar to that seen in other studies of R domain proteins (16, 30).

Earlier work showed that R1 (CFTR residues 645–834) stimulated CFTR-ΔR/S660A channel activity in excised membrane patches (13). Fig. 3 shows that adding phosphorylated R8 to the cytosolic surface of CFTR-ΔR/S660A reversibly stimulated current 33.4 ± 3.7% ($n$ = 9). This stimulation is similar to that which we previously reported with the R1 construct (43.2 ± 3.4%) (13). The small difference may be caused by the presence of Ser-660 in R1. Like wild-type CFTR, current depended on ATP (Fig. 3). Nonphosphorylated R8 had no effect, consistent with an earlier study showing no effect of nonphosphorylated R1 (13). Similar results were obtained with both NMDG-Cl and NaCl buffers. These data indicate that purified recombinant R8 retains stimulatory activity and that stimulation requires phosphorylation.

**Structural Studies of R8.** Sedimentation equilibrium showed that soluble R8 was a monomer, both phosphorylated and nonphosphorylated (Fig. 4).

We used limited proteolysis to determine whether portions of R8 would be inaccessible to proteases, suggesting conformational protection. We chose proteases with multiple potential consensus sites within R8, trypsin (10 sites), and papain (3 sites), which are evenly distributed throughout the protein. The tryptic patterns of phosphorylated and nonphosphorylated R8 (Fig. 5*A*) show that most of the protein is susceptible to trypsin. Similar results were found after papain digestion (Fig. 5*B*). In addition, the tryptic pattern after an 80-min digestion was similar in phosphorylated and nonphosphorylated R8 after correcting for the size difference because of phosphorylation. We sequenced proteolytic fragments from nonphosphorylated R8 and found fragments that corresponded to most of the predicted proteolytic sites. For example, trypsin cut at R810/811, R792, and R764/765/766. We also sequenced three proteolytic fragments from phosphorylated R8 that corresponded to nonphosphorylated R8 (Fig. 5). These data suggest that most of R8 was accessible to both proteases and that phosphorylation did not induce a global

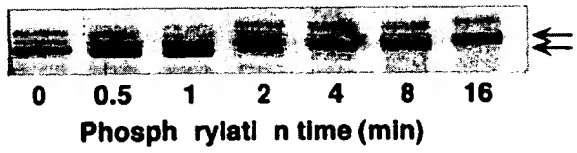


Fig. 2. Effect of phosphorylation on electrophoretic mobility of R8. R8 was phosphorylated with PKA and ATP at 30°C for time indicated and electrophoresed on SDS/PAGE. Arrows indicate nonphosphorylated and phosphorylated R8.

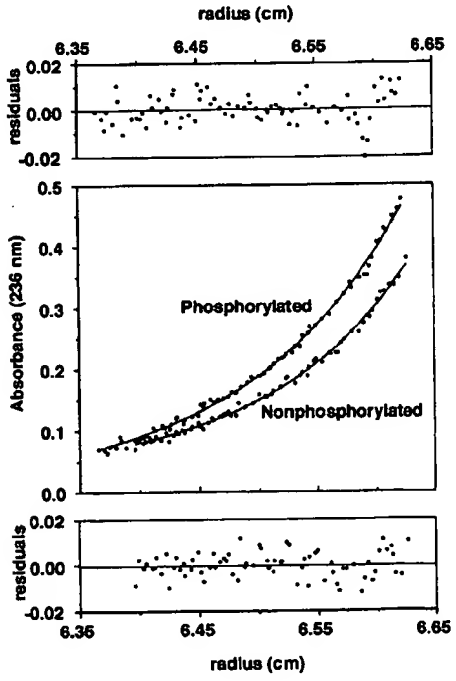


Fig. 4. Sedimentation equilibrium ultracentrifugation of R8. Smooth lines (*Middle*) are fit of data to Eq. 1. Fitted molecular weight for nonphosphorylated R domain is 16,640 ± 680 and $A_0$ = 0.022; that for phosphorylated R domain is 15,250 ± 470 and $A_0$ = −0.003. Predicted molecular weight of nonphosphorylated R8 based on amino acid composition is 15,270. Residuals of fit are shown (*Top* and *Bottom*) for phosphorylated and nonphosphorylated R8, respectively.

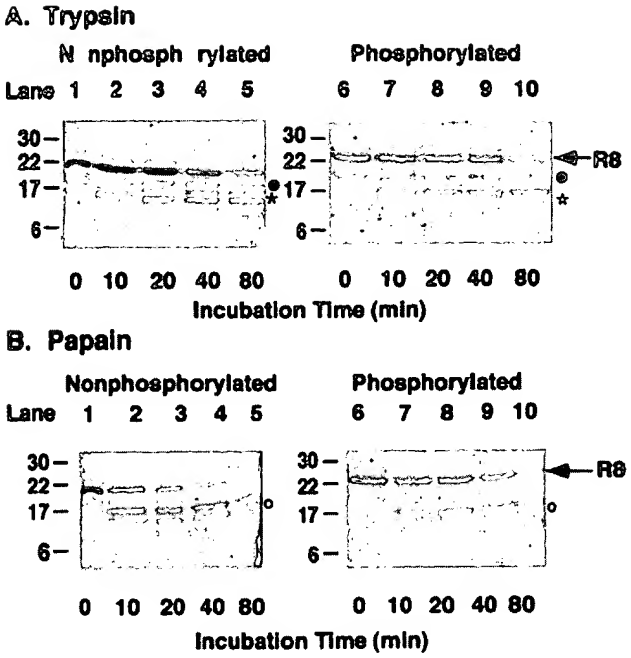


Fig. 5. Proteolytic patterns of R8. Equal amounts of R8 were incubated with either trypsin or papain for indicated times. Lanes 1–5 are nonphosphorylated and lanes 6–10 are phosphorylated R8. Arrow indicates intact R8. Sequences of indicated proteolytic fragments are: (⊛) GIRKFS1; (*)RQSVLNLM; and (○)SVNQGQNI.

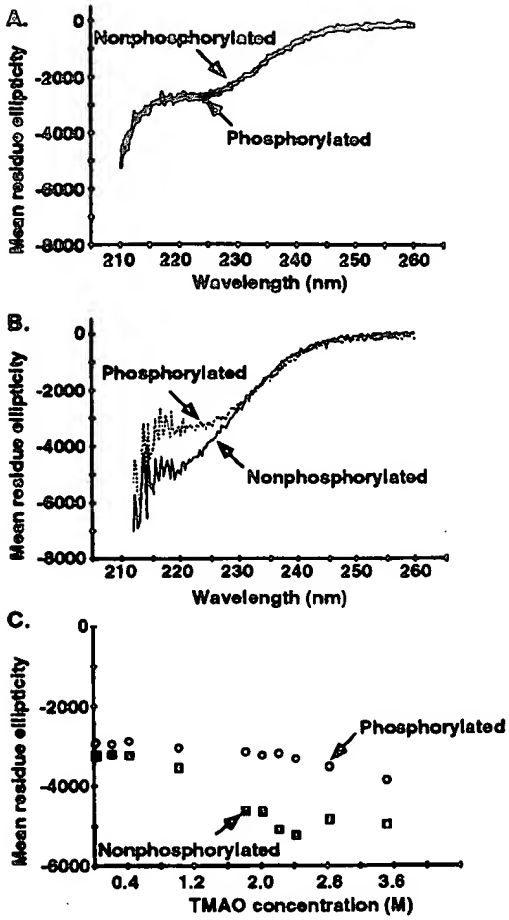


Fig. 6. CD spectra of R8. (*A*) R8 (0.15 mg/ml) in 10 mM $KP_i$, pH 7.3. (*B*) R8 (0.15 mg/ml) dialyzed into 2.8 M TMAO. Other conditions were similar to those in *A*. Spectra extend only to 210 nm because TMAO interferes with signal below 210 nm. (*C*) Equal concentrations of phosphorylated and nonphosphorylated R8 (0.15 mg/ml) in 1 mM glycine, pH 9.0, were diluted into increasing concentrations of TMAO and ellipticity measured at 220 nm.

conformational change in R8, but they do not eliminate the possibility of small discrete changes undetectable by these methods.

CD was used to examine the conformation of R8. Fig. 6*A* shows that R8 was a random coil with little well-ordered secondary structure. The results were the same irrespective of whether spectra were obtained in high pH, low salt, or the buffers used for patch clamp. The negative ellipticity at 222 nm is consistent with a helical content of about 5% (31) with the balance being random coil. Phosphorylated and nonphosphorylated R8 had similar CD spectra in the aqueous buffers (Fig. 6*A*), suggesting that phosphorylation did not induce a large structural change in R8.

We considered the possibility that interaction of R8 with lipid components of the plasma membrane might alter its conformation. To test this, we incorporated R8 in phospholipid micelles. This did not alter the CD spectrum.

To test whether R8 has the potential to fold, we examined the effect of TMAO. TMAO is a natural osmolyte that promotes folding of proteins; many unfolded proteins have been shown to adopt their native structure in TMAO (32). As shown in Fig. 6*B*, TMAO altered the CD spectra of nonphosphorylated R8 (compare Fig. 6 *A* and *B*), consistent with a small decrease in random coil and a modest increase in helical content to about 10%. This relatively small TMAO-induced increase in helical content was saturated at 2.8 M as shown by the TMAO titration curve (Fig. 6*C*). Interestingly, the helical content of phosphorylated R8 was only slightly increased in TMAO and was less than the change observed for nonphosphorylated R8 in TMAO. Thus, TMAO had only minimal effects on the secondary structure of R8; R8 retained a predominantly random coil conformation, whether phosphorylated or not.

## Discussi n

The data show that R8 (residues 708–831 of CFTR) is functional; it stimulated CFTR-ΔR/S660A channel activity. Surprisingly, R8 is predominantly unstructured, exhibiting a CD spectrum characteristic of random coil, both when phosphorylated and nonphosphorylated. Because R8, like wild-type CFTR, must be phosphorylated before it can activate CFTR-ΔR/S660A, either the phosphorylated R8 binds and stimulates CFTR while it is a random coil, or R8 adopts a more ordered structure on contact with the rest of CFTR. Interestingly, TMAO that promotes folding of other unstructured proteins had only minimal effects on R8.

The conclusion that the functional R domain is predominantly random coil is consistent with three other observations. First, we evaluated R8 with three structural prediction algorithms: Chou and Fasman (33), Profile Network Prediction of Secondary Structure (34, 35), and JPRED (36). The programs did not agree in the assignment of α-helix and β-sheet secondary structure. Second, the sequence of R8 is not well conserved in CFTR from different species (refs. 9 and 10 and unpublished work). Most highly structured proteins show substantial sequence conservation; examples are the NBDs of CFTR. Moreover, many of the conserved residues in such proteins have hydrophobic side chains buried within the protein core, where they help maintain structure (37). In contrast, the conserved sequences in R8 are the consensus PKA phosphorylation motifs, which are expected to

be solvent exposed where they can serve a functional rather than a structural role. Third, although more than 850 mutations have been reported in the CFTR gene [http://www.genet.sickkids.on.ca (1999) *Website*], there are relatively few missense mutations in the region encoding R8. Within exon 13, missense mutations have been observed in 17% of the codons in residues 590–708, but in only 6% of the codons in residues 708–830. From this region, the mutations R792G, A800G, E822K, and E826K increase or decrease current, but have not been reported to alter channel properties (38, 39). These observations are consistent with the notion that an amino acid change in a region that is predominantly random coil may be less likely to disrupt function and thereby cause CF.

Earlier studies of larger R domain proteins had suggested that the R domain adopts an ordered structure (30, 40). The CD spectrum of a construct (595–831) encoding most of exon 13 suggested a structural content of 10% $\alpha$-helix and 30% $\beta$-sheet (40). A study of an even larger construct (404–830) predicted 19% $\alpha$-helix and 43% $\beta$-sheet (30). Both of those constructs include significant portions of NBD1 based on sequence comparisons and the crystal structure of HisP (see Introduction and ref. 11). Therefore, it seems likely that the $\alpha$-helices and $\beta$-sheets were localized in NBD1 and the random coil was localized in the R domain. Thus, the results of those studies may not be so different from those reported here.

If phosphorylation does not increase R8 structure, how does it activate the channel? Phosphorylation might induce a conformational change only in discrete regions of R8, resulting in small spectral shifts masked by the larger signal from the random coil. Such discrete structural changes might be sufficient for a functional effect. Second, phosphorylation might simply introduce negative charge into R8. This interpretation would be consistent with the finding that mutation of phosphorylatable serines to aspartate activated the channel (19). Finally, phosphorylation may not directly change the conformation of R8, but may simply be required for an interaction of R8 with other sites within CFTR. Perhaps the regions immediately surrounding the conserved PKA phosphorylation sites are involved in interaction with and stimulation of CFTR.

This study also has some limitations. First, in the Introduction, we described the rationale for choosing the boundaries of R8. It could be that the actual boundaries of the R domain extend beyond residues 708–831. Importantly, however, more extensive deletions could not be made without destroying channel function. The ability to delete residues 708–831 and yet retain channel function, coupled with the ability of these same residues to partially restore phosphorylation-regulated activity, suggests that R8 represents a "functional" domain. Second, whereas our data indicate that R8 is primarily random coil even under conditions designed to allow folding, it is possible that R8 could adopt a more structured conformation in the presence of the rest of CFTR.

The advantages of unfolded proteins for signaling or regulation are becoming more apparent (41, 42). Examples include the cell-cycle kinase inhibitor $p21^{waf1/Cip1/Sdi1}$ (43), the FlgM flagellar protein of *Salmonella typhimurium* (44), and the fibronectin receptor-binding protein (45). The fast inactivation domain of the Shaker B $K^+$ channel acts in a structure-independent manner (46, 47). An R domain composed predominantly of random coil has an analogy in the kinase-inducible domain (KID) of the cAMP-responsive element-binding protein (CREB). Several structural parameters indicate that KID is unstructured (48–51). Like R8, serine phosphorylation of KID does not increase structure (48, 51). However, just as phosphorylation allows R8 to activate the $Cl^-$ channel, phosphorylation allows KID to bind and activate CREB-binding protein (CBP). This binding induces a conformational change in KID that is limited to the phosphoserine and a few neighboring amino acids (51, 52).

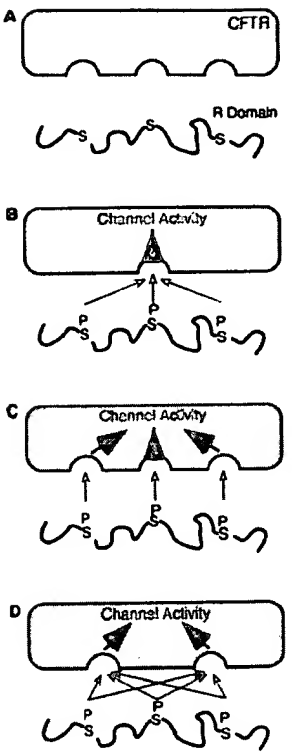


**Fig. 7.** Models of interaction of R domain with the rest of CFTR (in gray). See text for details.

An R domain that is predominantly random coil with a few conserved phosphorylation sites may explain some seemingly puzzling aspects of CFTR function. Earlier studies have shown that no single phosphorylation site is required for stimulation, that phosphorylation of several different sites can stimulate, and that not all phosphorylated sites have the same effect (6–8, 13, 15, 18–21). Fig. 7 shows some speculative models of how the R domain might stimulate CFTR and emphasize the functional advantages of an R domain with few structural constraints.

Model A shows the unphosphorylated R domain as random coil. Without phosphorylation, it does not stimulate activity.

Model B shows a phosphorylated R domain. Although we show three phosphoserines in the R domain, the actual number phosphorylated in an individual CFTR molecule is not certain. Because the R domain is unstructured, any of several different phosphoserines could interact with the single site shown on CFTR to stimulate channel activity. Model B could also explain the ability of multiple different phosphoserines to stimulate, possibly with quantitatively different effects on activity. However, this model does not explain how phosphorylation of more than one serine would give a graded increase in activity.

Model C shows multiple phosphoserines interacting with multiple sites in the rest of the protein. This model can account for increasing activity with increasing phosphorylation. Model C predicts that if there are three or four or five phosphoserines in the R domain, there must be three or four or five interaction sites for those phosphoserines. This model could also account for quantitatively different effects generated by phosphorylation of different serines.

Model D is the one we favor. This model shows multiple phosphoserines in the R domain interacting with multiple binding sites in CFTR. Although we do not know the number of sites with which the R domain interacts, here we show two, suggesting the possibility of at least one interaction site at each NBD.

However, there may be more interaction sites, as evidenced by the observation that regions within the R domain and the N terminus interact (53). Irrespective of the number of interaction sites, model D could account for the apparent promiscuous relationship between phosphorylation sites and stimulation of activity. In such a model, a relatively unstructured R domain would allow multiple different phosphoserines to stimulate, no one phosphoserine would be required, different phosphoserines could have quantitatively different effects, and the greater the degree of phosphorylation, the greater the activity.

The finding that the R domain is predominantly random coil is consistent with the evolving recognition that many protein domains and full length proteins are intrinsically unstructured (41, 42). It is also consistent with the emerging appreciation that unstructured proteins and domains hold certain advantages for signaling functions.

We thank Suzy Dietz, Lisa Einwalter, Pary Weber, and Theresa Mayhew for excellent assistance, Dr. Michael Winter for discussions, and Dr. James Walker for the pDC952 plasmid. We thank the University of Iowa DNA Core for sequencing help, and the University of Iowa Molecular Analysis Facility for protein sequencing and amino acid analysis. This work was supported by the National Heart Lung and Blood Institute (HL42385) and the Howard Hughes Medical Institute (HHMI). M.J.W. is an Investigator of the HHMI.

1. Riordan, J. R., Rommens, J. M., Kerem, B.-S., Alon, N., Rozmahel, R., Grzelczak, Z., Zielenski, J., Lok, S., Plavsic, N., Chou, J.-L., *et al.* (1989) *Science* **245,** 1066–1073.
2. Welsh, M. J., Tsui, L.-C., Boat, T. F. & Beaudet, A. L. (1995) in *The Metabolic and Molecular Basis of Inherited Disease*, eds. Scriver, C. R., Beaudet, A. L., Sly, W. S. & Valle, D. (McGraw–Hill, New York), pp. 3799–3876.
3. Tabcharani, J. A., Chang, X.-B., Riordan, J. R. & Hanrahan, J. W. (1991) *Nature (London)* **352,** 628–631.
4. Berger, H. A., Travis, S. M. & Welsh, M. J. (1993) *J. Biol. Chem.* **268,** 2037–2047.
5. Hwang, T.-C., Nagel, G., Nairn, A. C. & Gadsby, D. C. (1994) *Proc. Natl. Acad. Sci. USA* **91,** 4698–4702.
6. Wilkinson, D. J., Strong, T. V., Mansoura, M. K., Wood, D. L., Smith, S. S., Collins, F. S. & Dawson, D. C. (1997) *Am. J. Physiol.* **273,** L127–L133.
7. Gadsby, D. C. & Narin, A. C. (1999) *Physiol. Rev.* **79,** S77–S107.
8. Sheppard, D. N. & Welsh, M. J. (1999) *Physiol. Rev.* **79,** S43–S45.
9. Rich, D. P., Gregory, R. J., Cheng, S. H., Smith, A. E. & Welsh, M. J. (1993) *Recept. Channels* **1,** 221–232.
10. Dulhanty, A. M. & Riordan, J. R. (1994) *FEBS Lett.* **343,** 109–114.
11. Hung, L.-W., Wang, I. X., Nikaido, K., Liu, P.-Q., Ames, G. F.-L. & Kim, S.-H. (1998) *Nature (London)* **396,** 703–707.
12. Rich, D. P., Gregory, R. J., Anderson, M. P., Manavalan, P., Smith, A. E. & Welsh, M. J. (1991) *Science* **253,** 205–207.
13. Winter, M. C. & Welsh, M. J. (1997) *Nature (London)* **389,** 294–296.
14. Ma, J., Zhao, J., Drumm, M. L., Xie, J. & Davis, P. B. (1997) *J. Biol. Chem.* **272,** 28133–28141.
15. Cheng, S. H., Rich, D. P., Marshall, J., Gregory, R. J., Welsh, M. J. & Smith, A. E. (1991) *Cell* **66,** 1027–1036.
16. Picciotto, M. R., Cohn, J. A., Bertuzzi, G., Greengard, P. & Nairn, A. C. (1992) *J. Biol. Chem.* **267,** 12742–12752.
17. Cohn, J. A., Nairn, A. C., Marino, C. R., Melhus, O. & Kole, J. (1992) *Proc. Natl. Acad. Sci. USA* **89,** 2340–2344.
18. Chang, X.-B., Tabcharani, J. A., Hou, Y.-X., Jensen, T. J., Kartner, N., Alon, N., Hanrahan, J. W. & Riordan, J. R. (1993) *J. Biol. Chem.* **268,** 11304–11311.
19. Rich, D. P., Berger, H. A., Cheng, S. H., Travis, S. M., Saxena, M., Smith, A. E. & Welsh, M. J. (1993) *J. Biol. Chem.* **268,** 20259–20267.
20. Seibert, F. S., Tabcharani, J. A., Chang, X.-B., Dulhanty, A. M., Mathews, C., Hanrahan, J. W. & Riordan, J. R. (1995) *J. Biol. Chem.* **270,** 2158–2162.
21. Mathews, C. J., Tabcharani, J. A., Chang, X.-B., Jensen, T. J., Riordan, J. R. & Hanrahan, J. W. (1998) *J. Physiol.* **508,** 365–377.
22. Ramjeesingh, M., Li, C., Garami, E., Huan, L.-J., Galley, K., Wang, Y. & Bear, C. E. (1999) *Biochemistry* **38,** 1463–1468.
23. Ma, J., Tasch, J. E., Tao, T., Zhao, J., Xie, J., Drumm, M. L. & Davis, P. B. (1996) *J. Biol. Chem.* **271,** 7351–7356.
24. Price, N. C. & Johnson, C. M. (1989) in *Proteolytic Enzymes; A Practical Approach*, eds. Beynon, R. J. & Bond, J. S. (IRL, Washington, D.C.), pp. 163–180.
25. Matsudaira, P. (1987) *J. Biol. Chem.* **262,** 10035–10038.
26. Zamyatnin, A. A. (1984) *Annu. Rev. Biophys. Bioeng.* **13,** 145–165.
27. Laue, T. M., Shah, B. D., Ridgeway, T. M. & Pelletier, S. L. (1992) *Analytical Ultracentrifugation in Biochemistry and Polymer Science* (The Royal Society of Chemistry, Cambridge).
28. Hansen, J. C., Lebowitz, J. & Demeler, B. (1994) *Biochemistry* **33,** 13155–13163.
29. Spanjaard, R. A., Chen, K., Walker, J. R. & van Duin, J. (1990) *Nucleic Acids Res.* **18,** 5031–5036.
30. Neville, D. C. A., Rozanas, C. R., Tulk, B. M., Townsend, R. R. & Verkman, A. S. (1998) *Biochemistry* **37,** 2401–2409.
31. Scholtz, J. M., Qian, H., York, E. J., Stewart, J. M. & Baldwin, R. L. (1991) *Biopolymers* **31,** 1463–1470.
32. Baskakov, I. & Bolen, D. W. (1998) *J. Biol. Chem.* **273,** 4831–4834.
33. Chou, P. Y. & Fasman, G. D. (1978) *Adv. Enzymol. Relat. Areas Mol. Biol.* **47,** 45–148.
34. Rost, B. & Sander, C. (1993) *J. Mol. Biol.* **232,** 584–599.
35. Rost, B. & Sander, C. (1994) *Proteins* **19,** 55–72.
36. Cuff, J. A. & Barton, G. J. (1999) *Proteins* **34,** 508–519.
37. Bowie, J. U., Reidhaar-Olson, J. F., Lim, W. A. & Sauer, R. T. (1990) *Science* **247,** 1306–1310.
38. Wei, L., Vankeerberghen, A., Cuppens, H., Droogmans, G., Cassiman, J.-J. & Nilius, B. (1998) *FEBS Lett.* **439,** 121–126.
39. Vankeerberghen, A., Wei, L., Jaspers, M., Cassiman, J. J., Nilius, B. & Cuppens, H. (1998) *Hum. Mol. Genet.* **7,** 1761–1769.
40. Dulhanty, A. M. & Riordan, J. R. (1994) *Biochemistry* **33,** 4072–4079.
41. Wright, P. E. & Dyson, H. J. (1999) *J. Mol. Biol.* **293,** 321–331.
42. Plaxco, K. W. & Groß, M. (1997) *Nature (London)* **386,** 657–659.
43. Kriwacki, R. W., Hengst, L., Tennant, L., Reed, S. I. & Wright, P. E. (1996) *Proc. Natl. Acad. Sci. USA* **93,** 11504–11509.
44. Daughdrill, G. W., Chadsey, M. S., Karlinsey, J. E., Hughes, K. T. & Dahlquist, F. W. (1997) *Nat. Struct. Biol* **4,** 285–291.
45. Penkett, C. J., Redfield, C., Dodd, I., Hubbard, J., McBay, D. L., Mossakowska, D. E., Smith, R. A. G., Dobson, C. M. & Smith, L. J. (1997) *J. Mol. Biol.* **274,** 152–159.
46. Murrell-Lagnado, R. D. & Aldrich, R. W. (1993) *J. Gen. Physiol.* **102,** 949–975.
47. Murrell-Lagnado, R. D. & Aldrich, R. W. (1993) *J. Gen. Physiol.* **102,** 977–1003.
48. Richards, J. P., Bächinger, H. P., Goodman, R. H. & Brennan, R. G. (1996) *J. Biol. Chem.* **271,** 13716–13723.
49. Parker, D., Rivera, M., Zor, T., Henrion-Caude, A., Radhakrishnan, I., Kumar, A., Shapiro, L. H., Wright, P. E., Montminy, M. & Brindle, P. K. (1999) *Mol. Cell. Biol.* **19,** 5601–5607.
50. Radhakrishnan, I., Perez-Alvarado, G. C., Parker, D., Dyson, H. J., Montminy, M. R. & Wright, P. E. (1997) *Cell* **91,** 741–752.
51. Radhakrishnan, I., Perez-Alvarado, G. C., Dyson, H. J. & Wright, P. E. (1998) *FEBS Lett.* **430,** 317–322.
52. Parker, D., Ferreri, K., Nakajima, T., LaMorte, V. J., Evans, R., Koerber, S. C., Hoeger, C. & Montminy, M. R. (1996) *Mol. Cell. Biol.* **16,** 694–703.
53. Naren, A. P., Cormet-Boyaka, E., Fu, J., Villain, M., Blalock, J. E., Quick, M. W. & Kirk, K. L. (1999) *Science* **286,** 544–548.

# Communication

THE JOURNAL OF BIOLOGICAL CHEMISTRY
Vol. 265, No. 7, Issue of March 5, pp. 3599-3602, 1990


# Regulation of Isocitrate Dehydrogenase by Phosphorylation Involves No Long-range Conformational Change in the Free Enzyme*

(Received for publication, November 29, 1989)

**James H. Hurley‡, Antony M. Dean§, Peter E. Thorsness§‖, Daniel E. Koshland, Jr.§, and Robert M. Stroud‡¶**

*From the ‡Department of Biochemistry and Biophysics and Graduate Group in Biophysics, University of California, San Francisco, California 94143-0448 and the §Department of Biochemistry, University of California, Berkeley, California 94720*

**The structure of the phosphorylated form of isocitrate dehydrogenase from *Escherichia coli* has been solved and refined to an R-factor of 16.9% at 2.5-Å resolution. Comparison with the structure of the dephosphorylated enzyme shows that there are no large scale conformational changes and that small conformational changes are highly localized around the site of phosphorylation at serine 113. Tyrosine 160 rotates by 15°, and there is a local rearrangement of water structure. There is an 0.2-Å net movement of loop 230–234, and side chain shifts of 0.2 Å root mean square for isoleucine 159 and lysine 199. The lack of large conformational changes, the observation of a possible isocitrate binding site close to serine 113, and the demonstration that the phosphorylated enzyme is unable to bind isocitrate suggest that this enzyme is inactivated by a direct electrostatic interaction between the substrate and the serine phosphate.**

Protein phosphorylation is an ubiquitous post-translational modification of central importance in the regulation of many cellular processes (1), with phosphorylation at serine most common (2). Protein phosphorylation has long been known to have a key role in the control of metabolism in eukaryotes (1, 2) and in prokaryotes as well (3, 4). Despite the importance of protein phosphorylation in many aspects of cellular biology, only the regulation of one enzyme, glycogen phosphorylase, has previously been described structurally (5). Recently, the structure of isocitrate dehydrogenase (*threo*-D$_s$-isocitrate: NAD(P)$^+$ oxidoreductase (decarboxylating), E.C. 1.1.1.42) (IDH)[1] from *Escherichia coli*, an enzyme regulated by phosphorylation (4, 6), has been determined at 2.5-Å resolution (7). Phosphorylation of IDH, a functional dimer of 416-residue subunits, regulates the flux of substrate at a key branch point in carbohydrate metabolism (8–11) in response to changing nutritional conditions (8, 9, 12, 13).

Phosphorylation occurs at serine 113 (12, 14). In the three-dimensional structure of dephosphorylated IDH serine 113 is found in a pocket containing a number of positively charged and other polar residues which show a high degree of sequence conservation with isopropylmalate dehydrogenase (7). Although not yet solved with bound ligands, sequence conservation and charge distribution suggest that this pocket is the active site (7). Inactivation of IDH by phosphorylation occurs by preventing isocitrate from binding (15). Previous studies demonstrated that inhibition of binding is caused by the introduction of a negative charge at position 113 (14). These findings raise the question as to whether the mechanism of inactivation is through a direct electrostatic interaction between the phosphoserine and the negatively charged substrate isocitrate or if it is mediated by an induced conformational change. To address this question, we determined the structure of phosphorylated IDH and compared it with the structure of the dephosphorylated enzyme.

## EXPERIMENTAL PROCEDURES

IDH was phosphorylated *in vitro* by IDH kinase/phosphatase as described by LaPorte and Koshland (6), and crystals were grown essentially as for dephosphorylated IDH (7), except at 30% saturated ammonium sulfate instead of 34%. These grew to a size of 0.5 mm along the largest dimension and were isomorphous with the dephosphorylated crystals. Diffraction data were collected at room temperature on a Nicolet area detector using a laboratory CuK$\alpha$ rotating anode x-ray source and reduced with the XENGEN data reduction package.

The structure of phosphorylated IDH was determined by Fourier difference syntheses, using the dephosphorylated IDH model (7) as a parent structure. After the addition of water molecules placed in electron density at sites within 3.5 Å of potential hydrogen bond-forming groups, the parent structure was refined using minimization with XPLOR (16). A total of 110 water molecules with B-factors less than 50 have been kept in the current model, where $B = 8\pi^2\langle u^2\rangle_{rms}$, and $u$ is the displacement of an atom about its equilibrium position. Covalently bound phosphate was located at serine 113 in $(F_{pho} - F_c)\alpha_{calc}$ (Fig. 1) and $(F_{pho} - F_{dephо})\alpha_{calc}$ Fourier syntheses, with phases and amplitudes calculated from the dephosphorylated model. Phosphoserine was built into $(2F_o - F_c)\alpha_{calc}$ electron density with FRODO (17). The phosphorylated IDH model was refined with an effective solvent screening function of 20 to avoid an effect due to the lack of a solvation term in the empirical potential energy function used by XPLOR in which polar side chains with large B-factors form hydrogen bonds or salt bridges with nearby groups, although the electron density clearly indicates that these side chains project into the solvent. The net charge on the phosphoserine was set to zero, as with other charged groups. Water 557, displaced by the covalently bound phosphate group, was removed from the model prior to refinement with XPLOR. The R-factor of the phosphorylated model prior to refinement was 22.0%. Residues 3 and 4, which had not been placed in the parent structure, were located in electron density for the phosphorylated structure, probably due to the improved data for phosphorylated IDH. The phosphorylated structure was refined for four rounds of alternating minimization and manual rebuilding with the use of both $(F_o - F_c)\alpha_{calc}$ and $(2F_o - F_c)\alpha_{calc}$ Fourier syntheses.

* This work was supported by National Institutes of Health Grant GM 24485 (to R. M. S.), National Science Foundation Grant 04200 (to D. E. K.), Pittsburgh Supercomputer Center Grant DMB 890040P (to R. M. S.) for crystallographic refinement, and a University of California Regent's fellowship (to J. H. H.). Atomic coordinates of phosphorylated IDH have been deposited at the Brookhaven protein data bank. The costs of publication of this article were defrayed in part by the payment of page charges. This article must therefore be hereby marked "*advertisement*" in accordance with 18 U.S.C. Section 1734 solely to indicate this fact.

¶ To whom correspondence should be addressed.

‖ Present address: Section of Genetics and Development, Cornell University, Ithaca, NY 14853.

[1] The abbreviations used are: IDH, isocitrate dehydrogenase; rms, root mean square.

As the final phosphorylated structure appeared to be superior in quality to the parent model, the phosphoserine was replaced by serine, water 557 was put back in the model, and this structure was refined for two rounds of minimization and rebuilding against dephosphorylated amplitudes to produce an improved dephosphorylated IDH structure. Crystallographic statistics are summarized in Table I.

## RESULTS

The rms positional change for all main chain atoms (including $C_\beta$) between the two structures is 0.11 Å, less than the error in coordinates of either structure, estimated at 0.20 Å rms for $C_\alpha$ positions by the empirical formula $\Delta r = 0.5Rr$ of Stroud, where $R$ is the crystallographic R-factor and $r$ is the maximum resolution in angstroms (a further discussion of this formula will be published elsewhere). The mean coordinate error is approximately 0.40 Å for all atoms by the method of Luzzati (18). As the two structures were not solved independently, it is expected that the mean atomic shift is less than the mean coordinate error. The only significant positional changes are in the immediate vicinity of the phosphorylation site, as seen in Fig. 2. The conserved tyrosine 160 rotates by 15°, causing the hydroxyl oxygen to move by 0.9 Å, the largest movement of any protein atom. Isoleucine 159 moves by up to 0.3 Å (at $C_\gamma 2$), largely as a result of change in main chain torsion angles, and loop 229–234 undergoes a small concerted shift, with displacements of 0.1–0.6 Å. The entire loop undergoes a mean shift of 0.16 Å in the same direction, with an rms shift of 0.25 Å from the dephosphorylated structure. These movements appear to accommodate the new position of tyrosine 160. These changes, although similar in size or smaller than the estimated coordinate error, are clearly seen in $(F_{pho} - F_c)\alpha_{calc}$ and $(F_{pho} - F_{depho})\alpha_{calc}$ difference maps.

Lysine 199, which points into a large internal solvent-filled channel between the small and the clasplike domains of IDH and is in contact with the loop 229–234, also moves by up to 0.3 Å. This internal solvent pocket separates the phosphorylation sites on the two subunits, but displaced residues surrounding each phosphorylation site do not approach each other by less than 4.0 Å. Packing in and around the internal solvent-filled channel appears too loose to transmit a conformational change from one phosphorylation site to the other. This is in accord with the absence of cooperativity in the kinetics for phosphorylation of IDH by IDH kinase/phosphatase (6). Water 557 is replaced by the covalently bound phosphate, and there is a local rearrangement of water structure in the vicinity of residue 113. Water 417 moves by 1.5 Å; that this is the "same" water in both structures is signified by its unusually low B-factor of 10 and 11 in the phosphorylated and dephosphorylated structures, respectively. The identity of 417 is not well established but is modeled more reasonably as a water than as any of the ionic species (ammonium, sulfate, citrate, phosphate, sodium, chloride) present. The movement of water 417 closer to the covalently bound phosphate (from 3.9 to 3.4 Å) also brings it nearer to tyrosine 160 (from 4.2 to 3.6 Å) and may initiate the other small conformational changes.

TABLE I

*Crystallographic statistics for phosphorylated IDH (P-IDH) and dephosphorylated IDH (IDH)*

The crystallographic R-factor, $Rc = \Sigma|F_o - F_c|/\Sigma F_o$, is summed over all reflections with $|F|/\sigma(F) > 1$ from 5 to 2.5 Å; $F_o$ and $F_c$ are the observed and calculated amplitudes. $R_{merge} = \Sigma|I_i - \langle I\rangle|/\Sigma\langle I\rangle$, summed over all observations to 2.5 Å from four crystals.

| Space group $P4_32_12$ | $a = b = 105.1$ Å $c = 150.3$ Å | | | Resolution 2.5 Å | |
|---|---|---|---|---|---|
| | Reflections collected | Reflections, $F/\sigma(F) > 1$ | Observations collected | $R_{merge}$ | $Rc$ |
| P-IDH | 29,667 | 21,162 | 156,365 | 0.121 | 0.169 |
| IDH | 27,951 | 19,945 | 119,034 | 0.124 | 0.180 |

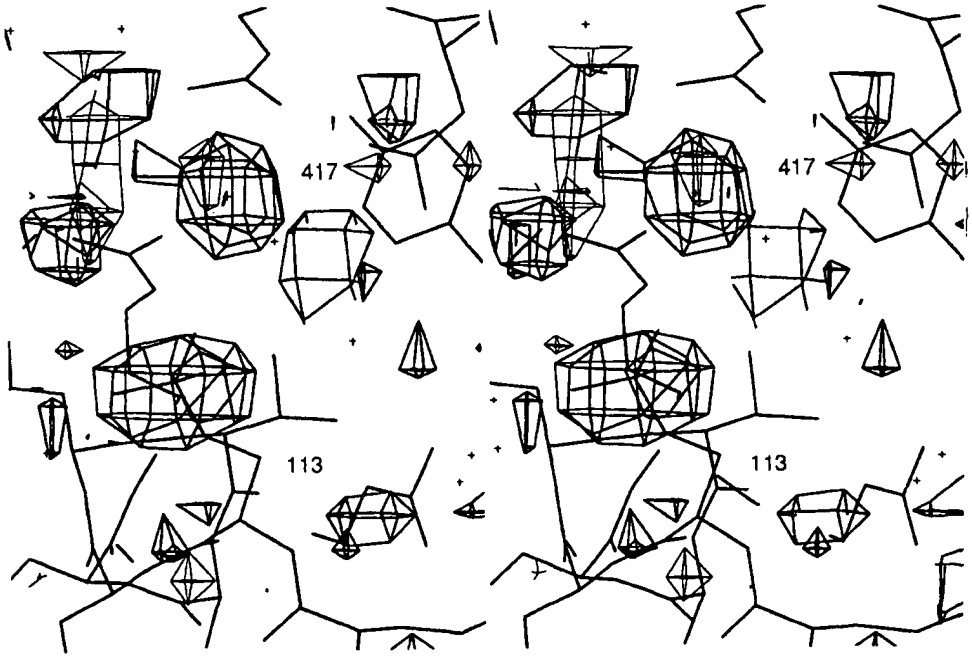


FIG. 1. **Region of residue 113 in positive difference electron density from a 2.5-Å $(F_o - F_c)\alpha_{calc}$ electron density map based on phases and amplitudes calculated from the dephosphorylated IDH model (7) and observed amplitudes for phosphorylated IDH.** The largest peak, with a peak height of 20 S.D., is for the covalently bound phosphate at residue 113; the other major peak seen represents the displacement of water 417.

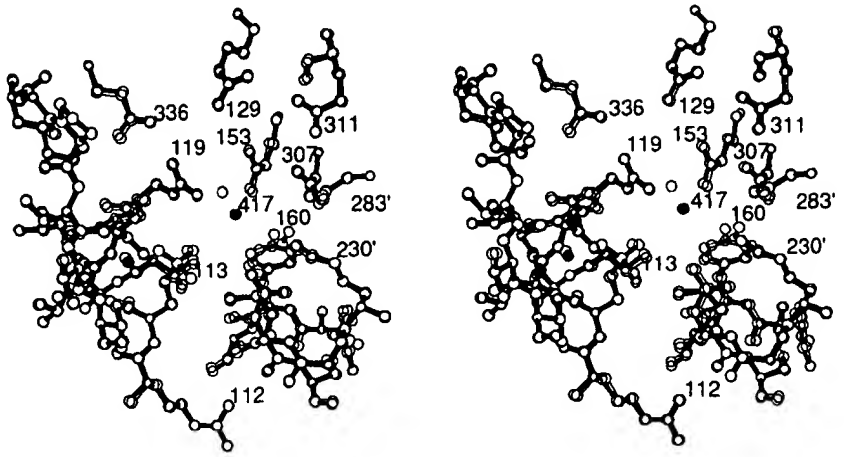


FIG. 2. **The environment of residue 113 viewed looking into the front pocket of IDH.** Phosphorylated IDH is shown with *solid bonds* and dephosphorylated IDH with *open bonds*. Portions of both subunits in the dimer are shown. Only water molecules which move by more than 0.2 Å between the two forms of IDH are shown. Waters of phosphorylated IDH are filled *black*, and waters of dephosphorylated IDH are *open*. Labeled residues include the conserved residues aspartates 283′ (the prime indicates the second subunit), 307, and 311, arginines 119, 129, and 153, glutamate 336, tyrosine 160, and lysine 230′. Also labeled are arginine 112, serine 113, and water 417.

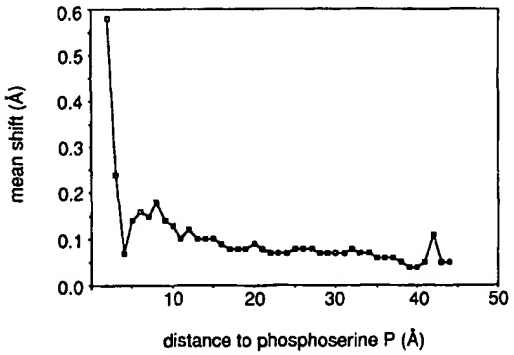


FIG. 3. **Mean atomic shift between the two forms of IDH as a function of distance to phosphoserine 113 P in phosphorylated IDH.** Shifts are plotted against the distance to the nearest of the two phosphorylation sites (one/subunit) in the IDH dimer. The mean shift rapidly decreases with distance from the phosphorylation site, approaching the overall value for the entire molecule at 10 Å from site 113.

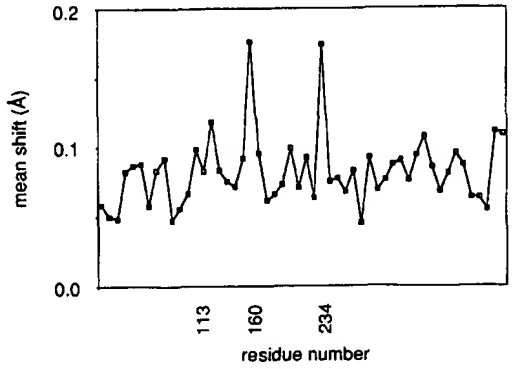


FIG. 4. **Mean atomic shift between the two forms of IDH averaged over 8 residues as a function of residue number.** Shifts are plotted against the central residue in the window of averaging. The largest shifts are restricted to the regions of residues 113, 160, and 234, close to the phosphorylation site in three-dimensional space.

Structural changes are highly localized in the region of the phosphorylation site (Figs. 3 and 4). Aside from the atoms mentioned above, near serine 113, no protein atom moves more than 0.4 Å. The pattern of atomic shifts between the two structures does not increase with B-factor (Fig. 5) and hence does not follow the pattern expected for shifts due to random positional errors (a general discussion of mean shift

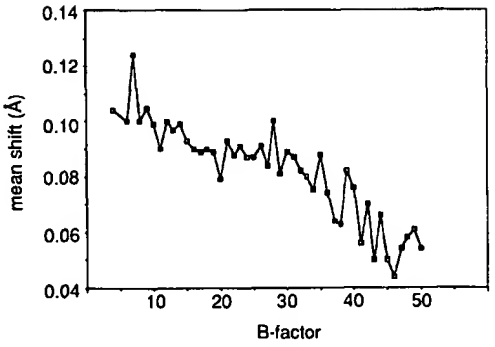


FIG. 5. **Mean atomic shift between the two forms of IDH as a function of B-factor.** B-factors are taken from the phosphorylated structure but are similar in both structures. The decrease in the mean shift with B-factor is contrary to the expected pattern for a distribution of changes due to random positional errors.

distributions and coordinates errors will be published elsewhere). The observation that there is actually a decrease in shift with increasing B-factor is due to the relatively low average B-factor in the region of serine 113.

## DISCUSSION

Because of the central importance of protein phosphorylation in biological regulatory systems, much effort has been invested in understanding how such covalent modifications alter protein function. In glycogen phosphorylase, phosphorylation of serine 14 initiates the glycogen phosphorylase *b* to glycogen phosphorylase *a* transition in which long-range conformational changes occur (5). In this transition, the thermodynamic equilibrium between conformational states along the activation pathway of the enzyme is shifted to more active conformations through effects both at distant allosteric effector sites and at the active site. In contrast to glycogen phosphorylase, which is activated by long-range conformational changes initiated by phosphorylation or allosteric effectors, IDH is inactivated by phosphorylation through an effect on substrate binding without any such long-range changes.

The location of the phosphorylation site in a pocket lined with highly conserved polar side chains and the lack of a large-scale conformational change in the unliganded enzyme on phosphorylation suggest IDH is inactivated by a direct electrostatic isocitrate-phosphoserine interaction. Alternatively, in the absence of a large conformational change upon phosphorylation, inactivation of IDH might proceed through small conformational changes if they were of sufficiently large

energy. Another possibility is that phosphorylation may prevent an induced conformational change necessary for substrate binding.

It may be asked whether lattice forces have prevented a solution-state conformational change involved in inactivation. Crystal packing interactions have occasionally had significant effects on protein structures. As phosphorylation reduces activity by at least 3 orders of magnitude (14), inactivation involves a free energy change of at least 4.5 kcal/mol. The lattice interaction energy is likely to be small in crystals of IDH, as these crystals are quite unstable, dissolving rapidly if placed in the well solution used in crystallization. It is thus likely that the free energy difference involved in inactivation is substantially larger than the lattice interaction energy and hence unlikely that the absence of a conformational change is an artifact of the crystalline state.

The structure of phosphorylated isocitrate dehydrogenase demonstrates that an enzyme can be phosphorylated in a functionally relevant way without a long-range conformational change. Thus the repertoire of known structural effects of regulatory covalent modification is increased. The diversity of possible structural effects of reversible covalent modifications of proteins produced by evolution is undoubtedly related to the great diversity of biological function of these modifications.

## REFERENCES


1. Krebs, E. (1986) in *The Enzymes* (Boyer, P. D., and Krebs, E. G., eds) 3rd Ed., Vol. 17, pp. 3–18, Academic Press, New York
2. Edelman, A. M., Blumenthal, D. K., and Krebs, E. G. (1987) *Annu. Rev. Biochem.* **56**, 567–613
3. Wang, J. Y. J., and Koshland, D. E., Jr. (1978) *J. Biol. Chem.* **253**, 7605–7608
4. Garnak, M., and Reeves, H. C. (1979) *J. Biol. Chem.* **254**, 7915–7920
5. Sprang, S. R., Fletterick, R. J., Goldsmith, E. J., Madsen, N. B., Acharaya, K. R., Stuart, D. J., Varvill, K., and Johnson, L. N. (1988) *Nature* **336**, 215–221
6. LaPorte, D. C., and Koshland, D. E., Jr. (1983) *Nature* **305**, 286–290
7. Hurley, J. H., Thorsness, P. E., Ramalingam, V., Helmers, N. H., Koshland, D. E., Jr., and Stroud, R. M. (1989) *Proc. Natl. Acad. Sci. U. S. A.*, **86**, 8635–8639
8. Kornberg, H. L., and Madsen, N. B. (1957) *Biochim. Biophys. Acta* **24**, 651–653
9. Kornberg, H. L. (1966) *Biochem. J.* **99**, 1–11
10. Holms, W. H., and Bennett, P. M. (1971) *J. Gen. Microbiol.* **65**, 57–68
11. Wang, J. Y. J., and Koshland, D. E., Jr. (1982) *Arch. Biochem. Biophys.* **218**, 59–67
12. Borthwick, A. C., Holms, W. H., and Nimmo, H. G. (1984) *Biochem. J.* **222**, 797–804
13. LaPorte, D. C., Walsh, K., and Koshland, D. E., Jr. (1984) *J. Biol. Chem.* **259**, 14068–14075
14. Thorsness, P. E., and Koshland, D. E., Jr. (1987) *J. Biol. Chem.* **262**, 10422–10425
15. Dean, A. M., Lee, M. H. I., and Koshland, D. E., Jr. (1989) *J. Biol. Chem.* **264**, 20482–20486
16. Brunger, A. T., Kuriyan, K., and Karplus, M. (1987) *Science* **235**, 458–460
17. Jones, T. A. (1985) *Methods Enzymol.* **115**, 157–170
18. Luzzati, P. V. (1952) *Acta Crystallogr.* **5**, 802–810